

# EXPERIMENTS ON LADDERS REVEAL A COMPLEX INTERPLAY BETWEEN A SPIN-GAPPED NORMAL STATE AND SUPERCONDUCTIVITY

Elbio DAGOTTO

*National High Magnetic Field Lab and Department of Physics, Florida State University, Tallahassee, FL 32306, USA  
By invitation for Reports of Progress in Physics*

In recent years, the study of ladder materials has developed into a well-established area of research within the general context of Strongly Correlated Electrons. This effort has been triggered by an unusual cross-fertilization between theory and experiments. In this paper, the main experimental results obtained in the context of ladders are reviewed from the perspective of a theorist. Emphasis is given to the many similarities between the two-dimensional high- $T_c$  cuprates and the two-leg ladder compounds, including  $\text{Sr}_{14-x}\text{Ca}_x\text{Cu}_{24}\text{O}_{41}$  (14-24-41) which has a superconducting phase at high pressure and a small hole density. Examples of these similarities include regimes of linear resistivity vs temperature in metallic ladders and a normal state with spin-gap or pseudogap characteristics. Some controversial results in this context are also discussed. It is remarked that the ladder 14-24-41 is the first superconducting copper-oxide material with a non-square-lattice layered arrangement, and certainly much can be learned from a careful analysis of this compound. A short summary of the main theoretical developments in this field is also included, as well as a brief description of the properties of non-copper-oxide ladders. Suggestions by the author on possible experiments are described in the text. Overall, it is concluded that the enormous experimental effort carried out on ladders has already unveiled quite challenging and interesting physics that adds to the rich behavior of electrons in transition-metal-oxides, and in addition contributes to the understanding of the two-dimensional cuprates. However, still considerable work needs to be carried out to fully understand the interplay between charge and spin degrees of freedom in these materials.

## CONTENTS

<b>1. Introduction</b> .....	1
<b>2. Theoretical Aspects: a Brief Summary</b> .....	3
2.1 Undoped Spin Ladder Models.....	3
2.2 Hole-doped Spin Ladder Models.....	4
<b>3. Experimental Results</b> .....	5
3.1 The Cu-oxide Ladder Compound $\text{SrCu}_2\text{O}_3$ .....	5
3.1.1 Doping of $\text{SrCu}_2\text{O}_3$ with Zinc.....	6
3.2 The metallic ladder compound $\text{La}_{1-x}\text{Sr}_x\text{CuO}_{2.5}$ .....	7
3.3 The Superconducting Ladder Compound $\text{Sr}_{14-x}\text{Ca}_x\text{Cu}_{24}\text{O}_{41}$ .....	8
3.3.1 Superconductivity in Doped 14-24-41 with $x=13.6$ .....	8
3.3.2 Superconductivity in Doped 14-24-41 with $x=11.5$ .....	9
3.3.3 Optical Conductivity $\sigma(\omega)$ .....	11
3.3.4 Nuclear Magnetic Resonance.....	12
3.3.5 Inelastic Neutron Scattering.....	13
3.3.6 Photoemission and Angle-Resolved Photoemission $A(\mathbf{p}, \omega)$ .....	13
3.4 The Strong-Coupling Ladder Compound $\text{Cu}_2(\text{C}_5\text{H}_{12}\text{N}_2)_2\text{Cl}_4$ .....	14
3.5 Vanadium-based Ladder Compound $\text{CaV}_2\text{O}_5$ .....	14
3.6 The Ladder Compound $\text{KCuCl}_3$ .....	15
<b>4. Conclusions</b> .....	15
<b>5. Acknowledgements</b> .....	16

## I. INTRODUCTION

The theoretical and experimental study of materials with an ionic structure containing dominant patterns in the shape of “ladders” has recently attracted a considerable attention in the context of Strongly Correlated

Electrons and Condensed Matter physics. The  $n$ -leg ladders are defined as  $n$  parallel chains of ions, with bonds among them such that the interchain coupling is comparable in strength to the couplings along the chains. The particular case of  $n=2$  motivates the use of the name “ladder” for this geometry. The coupling between the

two chains that participate in this structure is through “rungs”, language also extended to the  $n$ -leg systems. A vast literature on this subject has already accumulated, especially in the last three years. This made the study of ladders one of the two “hottest” topics of research in Condensed Matter for 1996 (see Grevin, Birgeneau and Wiese, 1997; Levy, 1996) and investigations in this area continue at a rapid pace.

What is the cause for this sudden interest on ladder systems? There are basically two broad reasons that have triggered the present enthusiasm on the subject. First, ladders provide a “playground” for studies of high critical-temperature ( $T_c$ ) superconductors (Bednorz and Müller, 1986) since in the absence of hole carriers they have a *spin-gap* in the energy spectrum, namely it costs a finite amount of energy to create spin excitations above the ground state, the latter being a spin-singlet. This property resembles the spin-gap feature that has been observed in the high- $T_c$  cuprates, particularly in the underdoped regime of low hole-density. Actually, for the two-dimensional (2D) cuprates a “pseudogap” is a better term for this feature since low-energy spin excitations exist, although with low spectral weight in neutron scattering experiments. Since at hole concentrations below the optimal value the normal state above  $T_c$  presents such a pseudogap, it is expected that its existence should be important for the superconductivity that occurs once the temperature is reduced below  $T_c$ . However, no clear consensus has been reached on the origin of the pseudogap in the 2D cuprates. In this framework, the ladder systems provide an interesting simpler setup for the analysis of spin and charge excitations in a spin-gapped environment since these systems certainly have a gap, both in theoretical calculations as well as real experiments, as discussed below.

Adding to this interesting spin-gap property, the early theoretical studies of ladders showed that upon doping of holes the ground state becomes dominated by *superconducting* correlations, as explained in the next section. Then, the analogy with the underdoped high- $T_c$  cuprates is even stronger, since the ladders not only share with them the presence of a spin-gap but also superconductivity is expected at a low-concentration of holes. Moreover, theory predicts that this superconductivity for ladders should be in the d-wave channel, the currently most accepted channel for superconductivity in the high- $T_c$  cuprates, adding further evidence for strong similarities between doped-ladders and doped-planes. Last but not least, ladders systems are considerably easier to study theoretically than two-dimensional models because they are basically quasi-one-dimensional. A plethora of powerful many-body techniques, notably those involving computational methods, work well in one-dimension but loose their accuracy in two-dimensions (Dagotto, 1994). Currently it is believed that the physics of isolated two-leg ladders is under reasonable theoretical control, and there is little controversy on its main properties.

The second motivation for the sudden interest in ladder

systems is related with the explicit realization of ladder compounds reported in seminal experimental papers reviewed here. The motivation provided by the theorists triggered an enormous effort on the experimental front to synthesize ladder materials, searching for the two main predictions made before those experiments, namely the existence of a the spin-gap and superconductivity. As shown below and after a considerable effort, clear evidence has already accumulated that real ladder materials with an even number of legs, two in particular, have a finite spin-gap in their spectrum of spin excitations in agreement with the theory. In addition, superconductivity in one of the ladder compounds has been detected upon the introduction of hole carriers and using high pressure. It is certainly tempting to associate this superconducting phase once again with the early predictions made by theorists in this context. However, it is fair to say that the origin of superconductivity in ladders is still actively under investigation and a consensus on this subject has still not been reached. Of particular current interest is the possible relevance of the interladder coupling to stabilize the superconducting phase. Thus, it remains to be investigated whether this phase corresponds or not to the theoretical predicted superconductivity based on the analysis of isolated ladders. In addition, several recent experiments have revealed additional close analogies between superconducting ladder compounds and high- $T_c$  superconductors. Adding to the spin-gap and superconducting properties, it has been observed that there are regions of parameter space where the resistivity of ladders is *linear* with temperature, a hallmark of the exotic normal state found in the two-dimensional cuprates.

The large number of experiments already carried out in the context of ladder materials and their many common features has motivated the presentation of this review. The paper is focussed on the *experiments*, aside from a brief summary of the main theoretical results in the next section, and it certainly does *not* attempt to review the huge literature accumulated in recent years on theoretical studies of ladder compounds. Such a formidable task is postponed for a future, more comprehensive, review article. The organization of the present paper is in sections that individually summarize the main results corresponding to particular ladder materials. Particular emphasis is given to copper-oxide based ladders, since some of them accept hole doping and the physics of carriers in spin-gapped backgrounds can be studied. However, other compounds are also described in the present paper. Comments by the author on some experiments are included in the text, and a comprehensive summary is provided in the last section of the review. The overall conclusion is that the study of ladders has already provided several interesting results to the experts in Strongly Correlated Electrons, and further work in this context should certainly be encouraged, especially regarding the clarification of the properties of its superconducting phase.

## II. THEORETICAL ASPECTS: A BRIEF SUMMARY

### 2.1 Undoped Spin Ladder Models

After a plethora of theoretical studies of the  $S=1/2$  Heisenberg model with interactions between nearest-neighbor spins, it has been clearly established that in two-dimensions and zero temperature the ground state is “antiferromagnetic” on a square lattice. This means that the “staggered” spin-spin correlations between spins at distance  $r$  decay to a nonzero constant as  $r$  grows. Here a modulating sign  $+1$  or  $-1$  for even and odd sites, respectively, is used in the definition of the staggered spin correlation. The decay to a finite constant at large distances indicates that the ground state has long-range order in the spin channel. In one-dimension (1D) quantum fluctuations are sufficiently strong to prevent such a long-range order, but the staggered spin-spin correlations decay slowly to zero as a power-law and they remain dominant. Both in 1D and 2D there is no spin-gap, namely there is no cost in energy to create a spin excitation with  $S=1$ .

The current interest in the study of ladder systems started when Dagotto, Riera and Scalapino (1992) found that the  $S=1/2$  Heisenberg model defined now on a two-leg ladder instead of a chain or a plane, has a *finite* spin-gap in its spectrum of spin excitations (see also Dagotto and Moreo, 1988). The reason leading to this result is simple in the “strong coupling” or “strong rung” limit, namely the limit where the Heisenberg coupling along the rungs ( $J_{\perp}$ ) is much larger than along the legs ( $J$ ). In this case, the ground state of the two-leg Heisenberg model corresponds to the direct product of spin-singlets, one per rung, as schematically represented in Fig.1a. The overall spin of the system is 0, since each rung pair of spins is itself in a singlet. In order to produce a spin excitation, a rung singlet must be promoted to a rung triplet, and this costs an energy  $J_{\perp}$ . These local excitations can propagate along the ladder and its energy acquires a momentum dependence (see Barnes et al., 1993). The spin-gap is the minimum at momentum  $\pi$ . Then, in the strong-coupling limit the spins are mostly uncorrelated, being in singlets most of the time, and the spin correlations decay with distance exponentially along the chains. Such a state is usually referred to as a “spin-liquid”. Gopalan, Rice and Sigrist (1994) and Noack, White and Scalapino (1994) suggested that a good variational description of the ground state can be obtained if the short-range resonance valence bond (RVB) state (Kivelson, Rokhsar and Sethna, 1987) is used. Note that this description is certainly accurate in the strong coupling limit, but in the isotropic limit it must be supplemented by spin-singlets among spins at distances larger than one lattice spacing to account for the observed correlation length of about three lattice spacings, obtained from the staggered spin-spin correlations (Noack, White and Scalapino, 1994).

Nevertheless, the short-range RVB-state is certainly a useful state to use in qualitative considerations of the physics of ladders. Other studies of ladders based on the RVB picture have also been presented by Sierra et al. (1998).

In the other limit  $J_{\perp} = 0$  the legs decouple and, as remarked above, it is well-known that isolated chains do not have a spin-gap and arbitrarily low-energy spin excitations can be created. However, these chains are in a “critical” state since they do not present long-range order but a power-law decay of correlations. It is anticipated that small perturbations may change qualitatively the properties of its ground state. Based on these considerations, Barnes et al. (1993) conjectured that a spin-gap opens on the two-leg ladders immediately upon the introduction of a nonzero  $J_{\perp}$ . Numerical results supported this proposal and the spin-gap was observed to be  $\sim J/2$  in the “isotropic” limit  $J = J_{\perp}$ , as also found numerically by Dagotto, Riera and Scalapino (1992). The actual spin-gap vs  $J_{\perp}/J$  is shown in Fig.2, using the frequently applied alternative notation  $J_{\perp} = J'$ . Similar results were obtained by White, Noack and Scalapino (1994). In addition, a spin-gap appears in the one-band Hubbard model at half-filling if defined on a two-leg ladder (see Noack, White and Scalapino, 1994; Azzouz, Chen and Moukouri, 1994). This result is reasonable since the Heisenberg model is recovered from the strong-coupling  $U/t$  limit of the one-band Hubbard model. Since the spin-gap is nonzero at all couplings with the only exception of  $J_{\perp} = 0$ , the “physics” of the two-leg ladders is said to be dominated by the strong-coupling limit with nearly decoupled rungs. Calculations in that regime are frequently carried out with the expectation that the results will not change qualitatively in the isotropic limit, which is more difficult to study directly due to the absence of a small perturbative parameter.

If the number of legs increases in the  $n$ -leg ladder structure, the physics of the two-leg ladders with its spin-gap should remain qualitatively the same as long as  $n$  is *even*. In this case, the strong coupling limit  $J_{\perp} \gg J$  leads once again to the formation of spin-singlets along the rungs since the ground state of  $n$  (even) coupled  $S=1/2$  spins has zero total spin. As a consequence, the excitation of  $S=1$  states costs a finite amount of energy. The gap must decrease with  $n$  such that the limit of a two-dimensional gapless plane is recovered as  $n$  grows, but its magnitude will remain nonzero for any finite  $n$  (even). Numerical calculations for the four-leg ladder by Dagotto and Moreo (1988); Poilblanc, Tsunetsugu and Rice (1994); and White, Noack and Scalapino (1994) support this picture. However, different is the situation if  $n$  is *odd*. If the strong coupling limit is studied, in each rung an odd number of spins must be considered and it is known that its ground state corresponds to a state with total spin  $S=1/2$ . Then, at large  $J_{\perp}$  the system can be mapped into a  $S=1/2$  one-dimensional Heisenberg model with a coupling among spins induced by a finite leg-coupling  $J$ . This system is gapless. As a consequence, these the-

oretical considerations, which were originally proposed by Rice, Gopalan and Sigrist (1993) and Gopalan, Rice, and Sigrist (1994), predict that odd-leg ladders should be gapless, while even-leg ladders have a finite spin-gap as discussed above (see also Rojo (1996)). Numerical calculations by White, Noack and Scalapino (1994) are in agreement with this prediction. Using a Monte Carlo loop algorithm and calculating the magnetic susceptibility as a function of temperature, Frischmuth, Ammon and Troyer (1996) also found evidence supporting the gapful vs gapless characteristics of the ground state of even- and odd-leg ladders, respectively. Their results are reproduced in Fig. 3.

## 2.2 Hole-doped Spin Ladder Models

The theoretical study of ladder models in the presence of hole doping leads to interesting predictions. Dagotto, Riera and Scalapino (1992) studied the t-J model on a two-leg ladder using computational techniques. In this model the degrees of freedom at each site are either a  $S=1/2$  spin that mimics the  $\text{Cu}^{2+}$  ion with 9 electrons in its d-shell or a “hole” that represents a  $\text{Cu}^{3+}$  state, usually assumed to be made out of a spin-singlet combination of an oxygen hole and the  $S=1/2$  copper-ion forming a so-called Zhang-Rice singlet. Analyzing the t-J model correlations corresponding to the operator that create or destroy hole pairs at nearest-neighbor sites and working at a small concentration of doped holes, Dagotto, Riera and Scalapino (1992) observed that these correlations were very robust, clearly indicative of a ground state dominated by strong superconducting tendencies. The rationalization of this surprising result is sketched in Fig.1b-c. The main idea is that the state upon which the holes are added is dominated by the formation of rung singlets, at least in strong-coupling. If a hole is added, equivalent to removing a  $S=1/2$ , the other spin of the original singlet becomes free and it no longer reduces its energy by singlet formation. If two holes at large distance are added to the system, each one will be producing a substantial energy damage to the spin background as sketched in Fig.1b since both break a singlet. However, if the two holes are nearby they can share a common rung, reducing the number of damaged spin singlets from two to one. This idea leads in a natural way to the concept of hole binding on two-leg ladders (Fig.1c). Once the formation of hole pairs is accepted as a logic consequence of the spin-singlet dominated characteristics of the undoped ground state, the presence of superconductivity becomes natural as explained by Dagotto, Riera, and Scalapino (1992) (see also Dagotto and Rice, 1996).

Sigrist, Rice and Zhang (1994) using a mean-field approximation predicted that the above described superconductivity in two-leg ladders should exist in the “d-wave” channel, namely the pair correlations should change sign if the creation (or destruction) hole-pair operator is aligned along the legs or along the rungs. Al-

though the two-leg ladder is certainly not invariant under rotations as the planes are, the language of referring to the superconductivity in ladders as “d-wave” is based on the similarities (sign change under rotations in  $90^\circ$ ) with the same concept used on square-lattices. Actually since the antiferromagnetic correlation length on ladders is about three lattice spacings, which is sufficiently large for the individual holes to be mainly surrounded by spins in an antiparallel arrangement, some of the arguments that lead to d-wave pairing in the 2D cuprates (see for instance Nazarenko et al., 1996) are also operative on ladders. This d-wave character of pairing on ladders has been confirmed by a variety of calculations performed by Riera (1994), Tsunetsugu, Troyer and Rice (1995), Hayward et al. (1995), and others. Some results are shown in Fig.4. Calculations in the one-band Hubbard model arrived to similar conclusions (see Asai (1994), Yamaaji and Shimoi (1994)). Additional information about hole binding can be found in Gayen and Bose (1995). Superconducting correlations have also been studied in three-leg ladders (Kimura, Kuroki, and Aoki, 1996a; Kimura, Kuroki and Aoki, 1996b). Very recently, Gazza et al. (1999) analyzed the hole binding and pairing correlations on two-leg ladders taking into account the Coulomb repulsion between carriers at distances of one lattice-spacing which is expected to be non-negligible. This interaction is rarely considered in the study of the t-J model. Gazza et al. (1999) found that in spite of this repulsion the binding and pair correlations are still robust on ladders, as it occurs when only on-site Coulomb interactions are included. This provides additional support to the idea that real doped ladders should be superconducting.

It is likely that these superconducting tendencies will be robust as long as the spin background does not alter drastically its spin-gap properties. However, it is also expected that the spin-gap will reduce its size as the hole doping increases (see Dagotto, Riera, and Scalapino, 1992; Noack, White and Scalapino, 1994; Poilblanc, Tsunetsugu and Rice, 1994; Hayward and Poilblanc, 1996). In this context, the spin excitations created upon hole doping were analyzed by Tsunetsugu, Troyer and Rice (1994). Besides the excitation that already appears in the undoped limit, namely the promotion of a rung spin-singlet to a triplet, other possible excitations may arise. For instance the hole pairs described in the previous paragraph may change their spin-singlet characteristics to a triplet. In other words, a bound state of a two-hole bound state and a rung spin-triplet may develop. The existence of this excitation has been recently confirmed by Dagotto et al. (1998) using a new technique that uses just a fraction of the total Hilbert space of a given cluster (Riera and Dagotto, 1993, and references therein), after the Hamiltonian is rewritten in the basis that diagonalizes the individual rungs. The undoped limit has also been studied in the plaquette-basis, instead of the rung-basis, as reported by Piekarewicz and Shepard (1997). A typical result in the rung-basis is shown in

Fig.5, working on a  $2 \times 16$  cluster. Of the two branches, one (I) is a remnant of the result observed without holes and the other one (II) is generated by hole doping and it corresponds to the hole-pair rung-triplet bound state. Other studies using the rung-basis have involved the calculation of the one-particle spectral function, and the results will be briefly summarized when photoemission experiments are discussed later in the review.

The list of interesting theoretical studies of ladder systems is certainly much longer than shown thus far in this section. Other aspects of ladder systems that have been analyzed in the literature include the careful study of antiferromagnetic correlation lengths vs temperature in the undoped limit (see Greven, Birgeneau and Wiese, 1996; Syljuasen, Chakravarty and Greven, 1997), weak coupling renormalization-group treatments (Kuroki and Aoki, 1994; Balents and Fisher, 1996a; Lin, Balents and Fisher, 1997; Lin, Balents and Fisher, 1998; Emery, Kivelson and Zachar, 1998), coupling of the chains with emphasis on the Luttinger liquid properties (Schulz, 1996), the influence of four-spin interactions in the undoped ground state (Nersisyan and Tsvelik, 1997), staggered spin ladders (Martin-Delgado, Shankar and Sierra, 1996), influence of disorder on ladders (Orignac and Giamarchi, 1998), two-leg Hubbard ladders and its relation with carbon nanotubes (Balents and Fisher, 1996b; Konik et al., 1998) and comparison with weak-coupling calculations (Park, Liang and Lee, 1998), influence of interladder coupling on the possible dimensional crossover of  $\text{Sr}_{14-x}\text{Ca}_x\text{Cu}_{24}\text{O}_{41}$  (Kishine and Yonemitsu, 1998), the relation between the resistivity of this material and the two-dimensional  $\text{YBa}_2\text{Cu}_4\text{O}_8$  cuprate (Moshchalkov, Trappeniers and Vanacken, 1998), as well as several others. In addition, ladder physics is also considered in the context of stripe phases for the two-dimensional cuprates since the region in between the presumed to exist one-dimensional-like metallic stripes are  $n$ -leg ladders. The spin-gap proximity effect discussed by Emery, Kivelson and Zachar (1997) proposes that a spin-gap is created in the 1D metallic striped environment due to the influence of a nearby system with spin-gapped properties, such as an even-leg ladder. The list of interesting ladder-related theoretical results goes on and on. However, since the focus of this review is on the experimental results found on ladder materials rather on theoretical developments, the author will postpone a comprehensive review of the latter for the near future and concentrate the efforts on the experimental aspects of ladder physics in the rest of the paper.

### III. EXPERIMENTAL RESULTS

After an enormous experimental effort, reviewed here, several materials with ladders in their structures have become available in recent years, and a variety of exciting experiments have already been carried out in this

context. In the present section the main experimental results will be discussed, organizing the presentation according to the family of ladder compound studied, and the technique used in its analysis. The main emphasis will be given to the Cu-oxide based ladders since they admit hole-doping by chemical substitution. Among them  $\text{Sr}_{14-x}\text{Ca}_x\text{Cu}_{24}\text{O}_{41}$ , the so-called “14-24-41” compound, will be discussed in particular detail since superconductivity has been found in this material, as described below. Note, however, that the compound that was mentioned in the early work of Dagotto, Riera and Scalapino (1992) as a possible realization of a ladder model was of a different variety, namely  $(\text{VO})_2\text{P}_2\text{O}_7$  (sometimes known as VOPO). This material, originally discussed by Johnston et al. (1987), has a two-leg V-oxide ladder in its structure. Neutron scattering experiments on VOPO presented by Eccleston et al. (1994) reported a spin-gap in the spectra which was interpreted in terms of a two-leg ladder dominant structure. However, more recent inelastic neutron scattering experiments by Garrett et al. (1997a) have shown that the properties of this compound are better described by an alternating Heisenberg antiferromagnetic chain, running perpendicular to the ladders (see also Garrett et al., 1997b). Based on this reanalysis, it is reasonable at present to assume that VOPO is no longer part of the family of ladder compounds, and thus the description below will be concentrated on other materials, notably those with chemical compositions containing copper and oxygen, similar to the high- $T_c$  cuprates, since they are susceptible to chemical substitutions and the concomitant addition of hole carriers.

#### 3.1 The Cu-oxide Ladder Compound $\text{SrCu}_2\text{O}_3$

A seminal contribution to the development of the field of ladders was provided by Azuma et al. (1994) (see also Hiroi et al. (1991)), when these authors reported the preparation of a copper-oxide  $S=1/2$  two-leg ladder. This result was not only important for providing a concrete realization of the ladder compounds discussed by the theorists, but also due to the possibility of changing the hole concentration through chemical substitution in such a Cu-oxide, as it occurs in the high- $T_c$  cuprates. The chemical composition of the compound reported by Azuma et al. (1994) was  $\text{SrCu}_2\text{O}_3$ , and a schematic representation is provided in Fig. 6. Note that within the ladders the  $180^\circ$  Cu-O-Cu bond should provide a strong Heisenberg coupling among the Cu-ions, while in between the ladders the bond is of  $90^\circ$  and, thus, expected to be weak and ferromagnetic.

In Fig. 7 the experimentally determined temperature dependence of the magnetic susceptibility of  $\text{SrCu}_2\text{O}_3$  is shown (from Azuma et al., 1994). The open circles are the experimental raw numbers, while as closed circles it is shown the data after subtraction of the Curie component due to impurities. The solid line through them is a theoretical fit that gives a spin-gap of 420K. This is in rough

agreement with the theoretical expectation of  $\Delta \sim J/2$  reported by Barnes et al. (1993), if it is assumed that the Heisenberg coupling is similar in magnitude to its two-dimensional copper-oxide counterpart  $J \sim 1200\text{K}$ . This is in principle a natural assumption due to the similarities between the Cu-O-Cu bonds on ladders and planes. Note that Azuma et al. (1994) also observed (Fig.8) that the magnetic susceptibility of a three-leg ladder material ( $\text{Sr}_2\text{Cu}_3\text{O}_5$ ) does not show indications of a spin-gap, as expected from a ladder with an odd number of legs (see Rice, Gopalan, and Sigrist, 1993; Gopalan, Rice and Sigrist, 1994; Sigrist, Rice, and Zhang, 1994; Dagotto and Rice, 1996). Muon spin relaxation measurements of the two- and three-leg compounds by Kojima et al. (1995) have also confirmed the gapful vs gapless character of the spin state of even- and odd-leg ladder systems. Recent experiments by Thurber et al. (1999) suggest that the three-leg ladder compound has a dimensional crossover from quasi-1D to anisotropic-2D at 300K.

$^{63}\text{Cu}$  Nuclear Magnetic Resonance (NMR) studies by Ishida et al. (1994) and Ishida et al. (1996) also contributed to the analysis of the two- and three-leg ladder compounds described here. The spin gap of  $\text{SrCu}_2\text{O}_3$  was in this case found to be 680K, i.e. larger than the result deduced from the magnetic susceptibility by Azuma et al. (1994), although of the same order of magnitude. The instantaneous spin-spin correlation was estimated to be 3-4 lattice spacings, in good agreement with theoretical expectations (White, Noack, and Scalapino, 1994, Dagotto and Rice, 1996, and references therein).

Regarding the difference between the spin-gap reported by magnetic susceptibility and NMR techniques, as well as the extra difficulty in understanding the origin of the actual value of the exchange Heisenberg constant which seems smaller than in other  $180^\circ$  Cu-O-Cu bond materials, Johnston (1996) made the important observation that the susceptibility data of  $\text{SrCu}_2\text{O}_3$  can be fit accurately with a two-leg ladder prediction using a rung coupling, denoted by  $J'$  in Fig.9, smaller by a factor two than the coupling along the legs  $J$  (see Barnes and Riera, 1994). Using the ratio  $J'/J \sim 0.5$ , the exchange constant needed to fit the data is now  $J \sim 2000\text{K}$  in agreement with results obtained for other cuprates by Motoyama, Eisaki and Uchida (1996) (for details see Johnston, 1996). Then, although the microscopic origin of the anisotropy between legs and rungs is still under discussion, evidence is accumulating that this compound corresponds to a ladder in the coupling regime  $J'/J < 1$  (note, however, that a ratio  $J'/J$  very close to 1 has been obtained by Matsuda et al. (1999) by including four-spin exchange interactions in the ladder model Hamiltonian to fit neutron scattering data for  $\text{La}_6\text{Ca}_8\text{Cu}_{24}\text{O}_{41}$ ). It is unclear to this author if for values of  $J'/J$  smaller than one superconductivity would be expected upon hole doping for realistic values of  $J/t$  in the t-J model discussed in the previous section. Calculations should be carried out in the interesting regime  $J'/J \sim 0.5$  to address this issue. Adding to the analysis of this material, Ishida et al. (1996) reported

the effect of doping carriers on the two-leg compound by substitution of Sr by La. Their results suggest that the added electrons unfortunately remain localized, and thus electron doped  $\text{SrCu}_2\text{O}_3$  may not provide a good realization of the physics arising from the (hole) doping of the t-J model. Other compounds are likely needed to realize the theoretical scenario discussed in Section 2.2.

### 3.1.1 Doping of $\text{SrCu}_2\text{O}_3$ with Zinc

The doping of  $\text{SrCu}_2\text{O}_3$  through the replacement of  $\text{Cu}^{2+}$  by  $\text{Zn}^{2+}$  has produced interesting results. Particularly important has been the observation by Azuma et al. (1997) of a rapid suppression of the spin-gap in this two-leg ladder compound as the concentration of Zn (here denoted by  $x$ ) was increased. The results for the magnetic susceptibility are shown in Fig.10. As  $x$  increases, the susceptibility also increases at low-temperature revealing the presence of low-energy spin states. At those temperatures an unexpected transition to an antiferromagnetic state is also observed, with a maximum Néel temperature of 8K. Then, it is apparent that a very small amount of impurities affects severely the low-temperature properties of  $\text{SrCu}_2\text{O}_3$  (see also Fujiwara et al., 1998). Recently, Ohsugi et al. (1998) reported a comprehensive study of  $\text{SrCu}_2\text{O}_3$  doped with Zn, Ni and La. The results were analyzed in terms of an impurity-induced staggered polarization around the vacancies. The size of this perturbation centered at, e.g., the Zn-ion was found to be very large, much longer than the 3-5 lattice spacings characteristic of the antiferromagnetic correlation length without the impurities. Actually the new correlation length is as large as 50 lattice spacings at Zn-doping  $x=0.001$ . Although rather surprising note that these results are qualitatively similar to those reported by Laukamp et al. (1998) using computational techniques in their study of the influence of vacancies on the spin arrangement in its vicinity, using two-leg ladders and neglecting interladder couplings. For Ni-doping similar theoretical results were obtained by Hansen et al. (1998). It is interesting to observe that a quite similar behavior has been found in spin-Peierls chains, which also have a spin-gap although of an origin quite different from the one found in ladders (for references on experiments and theoretical developments in this context see Laukamp et al., 1998). A possible rationalization of this curious phenomenon is the following: in the global spin-singlet state of the undoped ladder, it is known that the formation of local spin-singlets along the rungs is favored in the sense that such a configuration has a substantial weight in that ground state. If one of the spins is replaced by a zero-spin vacancy, such as  $\text{Zn}^{2+}$ , the other spin belonging to the same rung becomes “free” and, thus, it contributes to the magnetic susceptibility at low-temperatures as a  $S=1/2$  impurity would do. These impurities are certainly weakly interacting among themselves since their mean distance is large, but at very low-temperature such a residual interaction may nevertheless

favor a Néel order state, as discussed by Martins et al. (1996), Martins et al. (1997) and Laukamp et al. (1998). The reader should also consult the related literature contained in the work of Motome et al. (1996), Ng (1996), Nagaosa et al. (1996), Miyazaki et al. (1997), and references therein. Some of these authors also discussed the related *enhancement* of spin correlations in the vicinity of the vacancies, as observed in computational studies of spin systems for both ladders and dimerized chains. This enhancement favors the tendency towards antiferromagnetic order as the concentration of vacancies grows. As a consequence, from an apparently disordering effect such as the random replacement of Cu-ions by Zn-ions, an order state is stabilized at low-temperatures.

Laukamp et al. (1998) have also analyzed the ratio  $J_{\perp}/J$  that fits the data the best, and, in agreement with Johnston (1996), it was observed that a ratio 0.5 leads to an antiferromagnetic disturbance near the vacancies that covers the entire lattice even at very low Zn-concentrations. As example, the (staggered) local susceptibility calculated using numerical techniques is shown in Fig.11 for three values of  $J_{\perp}/J$ , namely 0.5, 1.0 and 5.28, the latter corresponding to the organic compound  $\text{Cu}_2(\text{C}_5\text{H}_{12}\text{N}_2)_2\text{Cl}_4$ , which will be discussed in another section of this review. Clearly at 0.5 is that all spins become involved in the staggered spin order at this vacancy density, a result compatible with experiments. The results in Fig.11 are actually very similar to the data in Fig.13 of Ohsugi et al. (1998) that reported the spatial variation of the antiferromagnetic moments in 1% and 2% Zn-doped  $\text{SrCu}_2\text{O}_3$ . Then, theoretical studies are able to reproduce the qualitative features of the experiments in ladders with vacancies.

### 3.2 The metallic ladder compound $\text{La}_{1-x}\text{Sr}_x\text{CuO}_{2.5}$

Under a high pressure of 6 GPa, Hiroi and Takano (1995) made the important discovery that the compound  $\text{La}_2\text{Cu}_2\text{O}_5$  undergoes a transformation into a simple perovskite structure. The ionic arrangement of this compound is shown in Fig.12. Two-leg copper-oxide ladders appear in the structure, involving  $180^\circ$  angle Cu-O-Cu bonds. The length and angle of the corresponding Cu-Cu bonds between ladders suggest that the interladder coupling is weaker than the intraladder one. Then, as a first approximation, it is reasonable to assume that this compound is formed by an array of weakly interacting two-leg ladders. More details about this material and the experiments can be found in the comprehensive review by Hiroi (1996). The temperature dependence of the magnetic susceptibility of  $\text{LaCuO}_{2.5}$  is shown in Fig.13, reproduced from Hiroi (1996). After removing the contribution of impurities, the resulting susceptibility indeed behaves as expected for a two-leg Heisenberg ladder. In particular, it presents a spin-gap behavior at low-temperatures with  $\Delta = 492\text{K}$ , a number similar to the gap obtained for  $\text{SrCu}_2\text{O}_3$  ( $\sim 400\text{K}$ ), as described in

the previous sections.

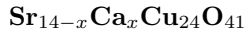
An important observation is that the ladder compound  $\text{LaCuO}_{2.5}$  can be hole doped replacing La by Sr (Hiroi, 1996). This doping is achieved also working at high pressure. There are no significant changes in the structure after doping. The amount of Sr that can be added to  $\text{LaCuO}_{2.5}$  is fairly large, up to  $x=0.20$ . Following this doping procedure a dramatic insulator-to-metal transition has been observed in the resistivity, as shown in Fig.14, taken from Hiroi (1996). Based on the sign of the slope of the resistivity vs temperature, the metal-insulator transition was found to be located roughly between  $x=0.18$  and 0.20. Note the sharp decrease in the resistivity with doping which corresponds to more than seven orders of magnitude. Comparing the results for this compound against those for the two-dimensional cuprate  $\text{La}_{2-x}\text{Sr}_x\text{CuO}_4$ , it was observed that at the hole density  $x \sim 0.20$ , the resistivities of both compounds are actually very similar, as the reader can observe in Fig.15 (Hiroi, 1996). The doping dependence of the magnetic susceptibility is contained in Fig.16. The spin-gap characteristics of the ground state seem to disappear with increasing doping. Photoemission and x-ray-absorption studies performed on  $\text{La}_{1-x}\text{Sr}_x\text{CuO}_{2.5}$  by Mizokawa et al. (1997) found changes in the overall electronic structure induced by hole doping similar to those in  $\text{La}_{2-x}\text{Sr}_x\text{CuO}_4$ . Spectral weight around the Fermi level ( $E_F$ ) was found to increase with  $x$ , and a weak but finite Fermi edge is established at  $x = 0.20$ . This result is compatible with the metallic character of the compound deduced from the resistivity at this hole concentration. Then, it is clear that  $\text{La}_{1-x}\text{Sr}_x\text{CuO}_{2.5}$  is a metal at  $x \sim 0.20$ , improving on the characteristics of  $\text{SrCu}_2\text{O}_3$  (Sec. 3.1) which is a two-leg ladder compound that cannot be hole doped.

Although the resistivity results presented in Fig.14 correspond to an encouraging metal-insulator transition upon doping, unfortunately those results also show that this ladder compound does not become a superconductor in spite of the theoretical predictions in this respect. There are two possible reasons to understand the absence of superconductivity here. First, the interladder coupling, while certainly smaller than the intraladder one, may not be negligible small since it does not involve  $90^\circ$  bonds. It is not clear to what extent this finite extra interladder coupling would change the theoretical predictions for isolated ladders. Second, the replacement of La by Sr produces an intrinsic randomness in the system that may localize the holes.

Regarding the first possibility, namely the relevance of the interladder couplings in this compound, Normand and Rice (1996) proposed that the magnetic state of  $\text{LaCuO}_{2.5}$  may be located in parameter space near the crossover from spin-liquid to the antiferromagnetic state expected on a three-dimensional spin system without frustration (see also Normand and Rice (1997)). This proposal is motivated by the NMR results of Matsumoto et al. (1996) and  $\mu\text{SR}$  results of Kadono et al. (1996) that actually reported the presence of antiferromagnetic

order in this compound at a temperature  $T_N \sim 110\text{K}$ . Then, it is apparent that the spin-singlet state is in close competition with a Néel state in this compound. Troyer, Zhitomirsky and Ueda (1997), using a combination of analytical and quantum Monte Carlo techniques, expanded on Normand and Rice’s idea and showed that the apparently conflicting experimental results, namely evidence of spin-liquid formation at intermediate temperatures and a Néel state at low-temperature, can be reconciled if the system is near a quantum critical point. However, more recently Normand, Agterberg and Rice (1998) argued that even including realistic interladder couplings, the doped  $\text{LaCuO}_{2.5}$  compound should present superconductivity, at least within the spin-fluctuation approximation. Then, these authors concluded that the random potential due to the replacement of  $\text{Sr}^{2+}$  by  $\text{La}^{3+}$  must be responsible for suppressing the superconducting phase, and suggested that more work should be devoted to the preparation of single crystals of this compound at low-doping values to search for indications of superconductivity, which is expected to be the strongest in such a regime of density according to their theoretical calculations. Overall, it is clear that the experimental analysis of the properties of this ladder compound should continue in order to clarify what causes the suppression of superconductivity, and to investigate what sort of metallic state is obtained near the spin-gapped regime that resembles the behavior of the 2D cuprates.

### 3.3 The Superconducting Ladder Compound



After the quite interesting first attempts described in Sections 3.1 and 3.2 to search for superconductivity in two-leg ladders, success was finally reached using the compound  $(\text{La}, \text{Sr}, \text{Ca})_{14}\text{Cu}_{24}\text{O}_{41}$ , the 14-24-41 or “phone number” compound. The synthesis of this material was initially reported by Mc Carron et al. (1988) and Siegrist et al. (1988). This compound contains 1D- $\text{CuO}_2$  chains,  $(\text{Sr}, \text{Ca})$  layers, and two-leg  $\text{Cu}_2\text{O}_3$  ladders as shown in Fig.17. A very important property of this material is that it can be synthesized at ambient pressure, contrary to some of the compounds described in previous Sections. In addition, a spin-gap was confirmed to exist in the  $\text{Sr}_{14}\text{Cu}_{24}\text{O}_{41}$  compound as shown, for example, using inelastic neutron scattering by Eccleston, Azuma, and Takano (1996). The nominal Cu valence for this material is +2.25, which arises from  $[2 \times 41(\text{Oxygens}) - 2 \times 14(\text{Sr})]/24(\text{Cu})$ , instead of just +2.0. This means that holes are already doped into the structure (“self-doped” system), similarly as it occurs in more familiar high- $T_c$  compounds such as  $\text{YBa}_2\text{Cu}_3\text{O}_7$ . Replacement of Sr by Na, which is in a 1+ state, is possible and NMR studies have been recently reported for this compound by Carretta, Ghigna, and Lascialfari (1998). However, in practice the substitution of Sr by Ca, both of them in a 2+ valence state, turned out to be more

efficient in providing carriers to the ladders since such a doping may alter the distribution between the chains and ladders of the already existing holes. Carter et al. (1996) in their important early investigations in this context indeed managed to replace Sr by Ca increasing by this procedure the number of hole carriers on the ladders-chains structure. These authors reported a decrease of the resistivity by this procedure, and interpreted their results as corresponding to the addition of extra holes to the chains instead of the ladders. However, the prevailing current point of view is that Ca-doping produces a rearrangement of holes, moving them into the ladders, as explained in detail in the subsequent sections. The discussion that follows on the notable 14-24-41 compound will be organized starting with the remarkable discovery of superconductivity, followed by a review of the results obtained in this context using a variety of experimental techniques.

#### 3.3.1 Superconductivity in Doped 14-24-41 with $x=13.6$

A crucial breakthrough in the field of ladders occurred when Uehara et al. (1996) discovered superconductivity in the  $x=13.6$  Ca-doped compound  $\text{Sr}_{0.4}\text{Ca}_{13.6}\text{Cu}_{24}\text{O}_{41.84}$ . To stabilize superconductivity Uehara et al. (1996) observed that a high pressure of 3 GPa is needed. This discovery substantially contributed to the current enormous effort devoted to the understanding of ladder compounds (Levy, 1996). The resistivity  $\rho$  vs temperature at several pressures is shown in Fig.18. The drop in  $\rho$  at the critical temperatures  $T_c$  is clear. There is an “optimal” pressure at which the  $T_c$  is the highest. More recent studies of  $\text{Sr}_{0.4}\text{Ca}_{13.6}\text{Cu}_{24}\text{O}_{41+\delta}$  by Isobe et al. (1998) reported the resistivity vs temperature shown in Fig.19. The results are very similar to those previously reported by Uehara et al. (1996). The hump centered at  $\sim 100\text{K}$  disappears at 5 GPa and the sample goes into a metallic regime. Note that the resistivity at  $x=13.6$  and high pressure changes from an approximate  $T^2$ -dependence near the optimal pressure to a linear dependence at higher pressures when superconductivity is suppressed (see Isobe et al., 1998). This is different from the behavior observed in the 2D high- $T_c$  compounds and also different from observation at other Ca concentrations. The critical temperature vs pressure from Isobe et al. (1998) is reproduced in Fig.20. The bell-like shape of the curve clearly resembles the well-known results for the 2D cuprates, if it is assumed that pressure is replaced by hole concentration. The optimal pressure is around 5 GPa, with an optimal  $T_c$  close to 14K. While this critical temperature is obviously lower than those reached in two-dimensional high- $T_c$  cuprates, it is nevertheless higher than those of typical metallic superconductors in spite of its low-carrier density. In addition, it is important to remark that this compound is the only known copper-oxide superconductor *without* two-dimensional planes. Then, independently of whether



this material provides or not a realization of the theoretical ideas based on two-leg ladders reviewed in Sec.2, it nevertheless provides a very interesting case for the analysis of superconductivity in copper-oxides in general.

After the report of superconductivity in doped 14-24-41, it became very important to verify that the structure at ambient pressure with clearly defined ladders and chains remains stable under the high pressure needed to induce the superconducting regime. In other words, pressure-induced structural changes could have occurred in the 14-24-41 material. This issue has been addressed recently by Isobe et al. (1998) using x-ray diffraction measurements on a  $x=13.6$  Ca-doped sample. Among the main results reported by these authors is the confirmation that indeed no serious structural changes take place in this compound under high pressure, and as a consequence it is safe to consider that the superconducting phase is related with the original ladder-chain structure observed at ambient pressure. The main effect of pressure apparently is to reduce the distance between the ladders and chains ( $b$  direction), as the evolution of the lattice constants with pressure shown in Fig.21 suggests. This result is representative of hard intraplane and soft interplane bindings. A similar conclusion is reached by analyzing the effect of Ca-doping upon the original Sr-based Ca-undoped phase, namely the interatomic distance ladder-chain was found to be reduced by Ca-substitution (see Ohta et al., 1997) leading to a redistribution of holes originally present only on the chains, as also discussed by Kato et al. (1996), Motoyama et al. (1997), Osafune et al. (1997), and Mizuno, Tohyama, and Maekawa (1997). According to Isobe et al. (1998), the most important role of high pressure for realizing superconductivity is the hole redistribution between chains and ladders. In addition, the resistivity along the  $a$ -axis decreases substantially with pressure enhancing the two-dimensional characteristics of the compound, as discussed extensively below.

### 3.3.2 Superconductivity in Doped 14-24-41 with $x=11.5$

After the discovery of superconductivity at Ca-concentration  $x=13.6$ , a similar phenomenon was also observed at  $x=11.5$  by Nagata et al. (1997). At 4.5 GPa the superconducting critical temperature at this Ca-composition was found to be 6.5 K (see inset of Fig.22 for more details). Very recent specific heat and neutron scattering studies by Nagata et al. (1998b,1999) have found that an antiferromagnetic phase with a Néel temperature  $T_N \sim 2\text{K}$  exists at this Ca-composition, both at low pressures and at pressures comparable to those that induce superconductivity. Then, in the temperature-pressure diagram antiferromagnetism and superconductivity are neighboring phases. The discussion of the complicated spin arrangement leading to the magnetic ordering can be found in Nagata et al. (1998b,1999). However, since  $T_c$  is appreciably larger than  $T_N$ , it is more reasonable

to continue assuming that the superconducting phase is more likely induced by the spin-gapped normal state that exists in these ladder materials.

In Fig.22a, the resistivity along the  $c$ -direction (legs) is shown at several pressures as a function of temperature. Indications of superconductivity below 10K have been found in the range from 3.5 GPa to 8GPa. It is interesting to note the *linear*  $T$ -dependence of  $\rho_c$  above 80K in the ambient pressure limit, similarly as it occurs in the 2D high- $T_c$  cuprates at optimal density. This linear behavior can also be observed in a wide range of pressures, but as the pressure increases a crossover to a  $T^2$ -dependence was found (see, for instance, the inset of Fig.4 of Nagata et al., 1998a). Actually at 8 GPa a Fermi-liquid  $T^2$ -dependent resistivity was observed between 50 K and 300K. The behavior reported in this compound is, thus, very similar to what occurs in the two-dimensional cuprates between the underdoped or optimal and overdoped regions. This similarity suggests that an increase of the pressure may correspond to an increase in the number of carriers on the ladder planes. The Fermi liquid behavior at large pressure in the region where superconductivity disappears suggests that a 2D Fermi liquid state is not favorable for superconductivity, as it occurs in the overdoped regime of the two-dimensional high- $T_c$  cuprates.

Nagata et al. (1997) also reported the resistivity  $\rho_a$  in the direction perpendicular to the legs, along the ladder rungs (Fig.22b). A semiconducting-like behavior is observed below 1.5 GPa, suggesting that the charge dynamics is essentially one-dimensional and carriers are confined within each ladder. However, above this pressure the system becomes metallic. It is likely that the two-dimensional character of the electronic state increases as the interladder coupling increases due to the application of pressure. Even more illustrative is the ratio  $\rho_a/\rho_c$  vs temperature at various pressures shown in Fig.23, reproduced from Nagata et al. (1997). At low pressure this ratio can be as large as 100, while at the pressure where the superconducting volume fraction is at its maximum,  $\rho_a/\rho_c$  reaches its minimum value  $\sim 10$ . This result suggests that at low pressure the carriers are confined on ladders, very similarly as holes are confined on the 2D planes of the high- $T_c$  cuprates, while as the pressures increases they become deconfined. However, it is somewhat surprising that at the highest pressure of 8 GPa, where the two-dimensional character should be maximized following the previous reasoning,  $\rho_a/\rho_c$  is now  $\sim 20$  i.e. twice the minimum reached at 4.5 GPa.

It is certainly important to study the qualitative effect of pressure on the physics of the ladder compound 14-24-41. In particular, it should be clarified what is the role of the interladder coupling in the appearance of superconductivity. Arai and Tsunetsugu (1997) have recently estimated the interladder hopping to be 5% to 20% of the intraladder hopping. However, it is unclear whether this number should be considered “small” or “large”. It could occur that under high pressure the quasi-1D charge dynamics is preserved and superconductivity develops

mainly within the ladders, with a minor role played by the interladder hopping amplitude. Another possibility is that the interladder coupling, presumably enhanced as the pressure grows, induces a dimensional crossover from 1D to 2D. In this scenario, it may simply occur that the ladders become an anisotropic two-dimensional copper-oxide system after the application of pressure. These issues have been recently addressed in more detail by Nagata et al. (1998a) and the interpretation they provide of their results seem to favor the second scenario, i.e. they consider that pressure makes the 14-24-41 compound quasi two-dimensional. They base their conclusion on the  $\rho_c$  and  $\rho_a$  resistivities shown in Fig.23. Along the  $c$ -direction and low-temperature the system changes from an insulator to a superconductor, similarly as observed in 2D cuprates upon Zn substitution (see Fukuzumi et al., 1996). Along the  $a$ -direction,  $\rho_a$  becomes metallic at 4.5 GPa.

Regarding the results of Nagata et al. (1998a) this author would like to bring to the attention of the readers similar results obtained experimentally for the two-dimensional high- $T_c$  compounds, in particular  $\text{YBa}_2\text{Cu}_3\text{O}_{7-y}$ . Takenaka et al. (1994) compared the resistivity along one of the directions of the CuO planes ( $a$ -axis) against the resistivity along the direction perpendicular to the planes, which in the high- $T_c$  cuprates is the  $c$ -axis. The results are shown in Fig.24. It is important to note that near the *optimal* critical temperature, where  $T_c$  is the highest, the resistivity in *both* directions  $a$  and  $c$  is metallic. Then, in this regime the holes seem to have been deconfined from the planes, and they can move coherently between planes. The anisotropy  $\rho_c/\rho_a$  of YBCO is shown in Fig.25. Close to the optimal oxygen concentration and at 100K this ratio is close to 50. Based on these numbers, it is difficult to avoid making a connection with the results obtained for the doped ladders. In that case at the optimal pressure around 4.0-4.5 GPa the resistivity in both directions (along the legs and rungs of the ladders) is metallic, and the ratio  $\rho_c/\rho_a$  is between 16 and 18. The difference between 50 for optimal YBCO and 16-18 for optimal 14-24-41 does not seem particularly large. In this author's opinion, the combination of these results is suggestive of an interesting common phenomenon taking place at optimal hole concentration both in ladders and planes. The best  $T_c$  is obtained in a regime where the charge becomes deconfined to a dimension higher by one with respect to the dimension of the dominant structure in the system, namely planes in the 2D cuprates and ladders in 14-24-41.

If this analogy is correct, this author believes that the doped ladder compound should present an "underpressure" or underdoped regime, with metallic behavior along the  $c$ -axis and semiconducting at low-temperature along the  $a$ -axis. Based on the recent results of Nagata et al. (1998a), such a regime could occur at pressures below 4.0 GPa. According to Nagata et al. (1998a) indications of superconductivity already occur at 3 GPa, and in this case the ratio  $\rho_a/\rho_c$  is 40, only about half the

maximum reached at ambient pressure. Although the here proposed underdoped regime would exist, if at all, in a very narrow window in pressure, the dependence of the ladder hole concentration with such a pressure is not accurately known and it may occur that changing from 3.0 to 4.0 GPa alters appreciably the number of carriers on the ladders. Of course, another possibility is an abrupt change from the insulator to an "overdoped" superconductor as it may happen in the 2D electron-doped NdCeCuO high- $T_c$  compound (S. Uchida, private communication). The author believes that the study of this conjectured underdoped regime would further contribute to the understanding of the analogies and differences between the ladder and planar cuprates.

Adding to this discussion, note that even if high pressure indeed increases the two-dimensional characteristics of the system at all Ca-concentrations where superconductivity is observed, still the x-ray experiments of Isobe et al. (1998) have shown that the structure remains the same, namely with a weak interladder-coupling and with nearest-neighbor ladders shifted by half a lattice spacing. This geometry certainly does *not* correspond to a square lattice, and in addition it is likely that the dominant physics will still arise from the individual ladders since they have the largest couplings and  $\rho_a/\rho_c$  much larger from one. In other words, if the superconductivity on ladders and 2D cuprates have a common origin, any mechanism proposed for the explanation of such a phase on the square-lattice high- $T_c$  cuprates cannot depend on the fine details of such a lattice structure since ladder compounds under pressure are also superconducting. Also note that a competing charge-ordered state, with hole pairs as building blocks, may affect the occurrence of superconductivity at low-pressure, and only at high-pressure the extra mobility in the direction perpendicular to the ladders stabilizes the superconducting state, which still could occur through a pairing mechanism taking place mostly on ladders. Then, the issue of the 1D vs 2D characteristics of the superconducting phase still is under much discussion, and this crucial issue should certainly be addressed by future experiments.

Very recently, exciting results by Balakirev et al. (1998) have added extra evidence of an unconventional behavior in doped ladders. These authors showed that charge transport in the non-superconducting state of  $\text{Sr}_2\text{Ca}_{12}\text{Cu}_{24}\text{O}_{41}$  shares three distinct regimes in common with high temperature superconductors, including an unexplained insulating behavior at low-temperatures in which the resistivity increases as the logarithm of the temperature. A similar regime was found previously in the 2D cuprates by Ando et al. (1995). The other two regimes correspond to a variable-range-hopping behavior at very low-temperature and a linear behavior above 150K, as already discussed elsewhere in the text. Boebinger et al. (1996) studying the high- $T_c$  superconductors in pulsed high magnetic fields found an insulator to metal crossover at low-temperature in  $\text{La}_{2-x}\text{Sr}_x\text{CuO}_4$ . The suppression of superconductivity by the magnetic

fields allowed them to analyze this insulator-metal transition below  $T_c$ . The study of the analog metal-insulator transition in magnetic fields strong enough to suppress superconductivity for the case of two-leg ladders 14-24-41 at high pressure would be an important experiment to carry out in the near future. Its main motivation would be to find out if such a transition occurs at the optimal pressure, similarly as it happens in the 2D cuprates at optimal hole-density.

### 3.3.3 Optical Conductivity $\sigma(\omega)$ :

The study of the possible transfer of holes from chains to ladders upon Ca-doping has been illuminated by experiments reporting the optical conductivity along the  $c$ -axis carried out by Osafune et al. (1997). They used single crystals of doped 14-24-41 with Ca-concentration up to  $x=11$ . At this hole density the  $c$ -axis resistivity is metallic above 80K, while for smaller densities the system is insulating at all temperatures below 300K. The analysis of Osafune et al. (1997) made possible to isolate the contributions of the ladders from those of the chains. These authors showed that holes are actually transferred from chains to ladders upon Ca-substitution, as explained below. This result is in agreement with the conclusions of several other studies.

Fig. 26 contains the optical conductivity along the  $c$ -axis obtained by Osafune et al. (1997) for several Ca-concentrations and even for an Y-doped sample ( $x=3$ ). It is clear from the figure that the conductivity in the low-energy region below 1.2 eV increases with  $x$ , while the charge-transfer spectral weight decreases, suggesting a transfer of weight similarly as it occurs in the 2D cuprates when an insulator parent compound is hole-doped (see, for instance, Uchida et al., 1991). The analogy between results for ladders and planes clearly suggests that Ca-doping produces a redistribution of holes, moving them from the chains to the ladders. If the holes would be populating the chains, substantially different results would be expected instead of the observed doping of a charge-transfer parent compound. In addition, the results found experimentally are similar to those found by numerical simulations of models for ladders by Hayward, Poilblanc and Scalapino (1996). The low-energy integrated optical conductivity up to  $\omega$ , namely  $N_{\text{eff}}(\omega)$ , is shown in Fig.27, and it also resembles results for the 2D cuprates. Based on these analogies, Osafune et al. (1997) estimated the concentration of holes on the ladders as a function of Ca-doping. The result is shown in the inset of Fig.27. At  $x=11$ , the nominal valence of Cu is 2.2, which corresponds to 0.2 holes per Cu on the ladders. Once again, these doping concentrations resemble those reached in the two-dimensional square-lattice cuprates.

Interesting recent results by Osafune et al. (1999) using optical techniques have contributed further to the understanding of doped ladder materials. These authors concentrated their efforts on the infrared part of the spec-

tra of single crystals 14-24-41 with  $x=8$  and 11, as representatives of the low- and high-doping regions of the ladders (having 0.16 and 0.20 holes per ladder-Cu, respectively, based on the previous analysis of Osafune et al. (1997)). The resistivity along the leg ( $c$ ) and rung ( $a$ ) directions is shown in Fig.28. At  $x=8$  both directions show an insulating-like behavior, while at  $x=11$  there is a range of temperatures where the system is metallic in the leg-direction and insulating in the rung-direction. An interesting feature in the  $a$ -axis optical conductivity  $\sigma_a(\omega)$  both at  $x=8$  and 11 is shown in Fig.29. A pseudogap in the low-frequency region appears upon lowering the temperature (see also Ruzicka et al., 1998). It is reasonable to expect that the insulating properties that exist in  $\rho_a$  vs  $T$  are related with this pseudogap, as it occurs in underdoped high- $T_c$  cuprates when the pseudogap and resistivity in the interplane direction are contrasted (see Homes et al., 1993). In addition, the NMR experiments of Magishi et al. (1998) showed that the temperature  $T^*$  at which a gap opens in the doped ladders coincides with the analogous temperature arising from  $\rho_a(T)$  data.

In contrast to the pseudogap in the  $a$ -direction, the  $c$ -axis optical conductivity  $\sigma_c(\omega)$  was found by Osafune et al. (1999) to be dominated by a low-frequency peak which rapidly grows with lowering temperature (Fig.30). This is not a Drude peak since it is located at a finite frequency  $\sim 100\text{cm}^{-1}$  and  $\sim 50\text{cm}^{-1}$  for  $x=8$  and 11, respectively. Osafune et al. (1999) have interpreted this result as arising from a charge-density-wave CDW mode of hole pairs. In addition, independent studies of the electrodynamics of  $x=0, 5$ , and 12 14-24-41 samples by Ruzicka et al. (1998) led to a similar proposal of a CDW of hole pairs at low-temperatures. Pseudogap features along the  $c$ - and  $a$ -axis were also observed by these authors. Also Owens, Iqbal and Kirven (1996) using microwave loss measurements detected superconductive pairing fluctuations close to a CDW instability. The proposed hole-pair CDW state is certainly possible since it is well-known from theoretical calculations that superconductivity and charge-ordering are competing states in many models (see Dagotto, Riera, and Scalapino, 1992; Noack, White and Scalapino, 1994; Tsunetsugu, Troyer and Rice, 1995). Indeed the effective mass that Osafune et al. (1999) obtained from their analysis is very large suggestive of the collective nature of the excitation. Thus, the proposed picture is that hole-pairs are formed and confined on the ladders, as predicted by theory, at small hole concentration. As the hole density grows they seem to form a CDW state of pairs. Upon increasing the hole concentration and working at intermediate temperatures the CDW may be depinned by thermal fluctuations and both pairs and single holes could contribute to the resistivity along the  $c$ -axis. Needless to say, it is very important to extend these results obtained at ambient pressure into the superconducting regime at high pressure, where both resistivities indicate a metallic behavior. Finally, note that very recent Cu-NQR and NMR experiments by Ohsugi et al. (1999) for the Ca( $x=11.5$ )

ladder have revealed three-dimensional magnetic ordering below  $T_N = 2.2\text{K}$ , with small moments appearing on the ladders and large moments on the chains. It was suggested that the CDW state of pairs plays an essential role in stabilizing the magnetic state.

### 3.3.4 Nuclear Magnetic Resonance:

A comprehensive Cu NMR study of single crystals of  $\text{Sr}_{14-x}\text{Ca}_x\text{Cu}_{24}\text{O}_{41}$  has been recently reported by Magishi et al. (1998). These authors analyzed the  $^{63}\text{Cu}$  NMR spectrum, Knight shift, nuclear spin-lattice relaxation rate  $1/T_1$ , and the spin-echo decay rate  $1/T_{2G}$  for samples with  $x = 0, 6, 9,$  and  $11.5$ . The main reported results emerging from this study are the following:

i) Through the Knight shift and  $1/T_1$  measurements, the spin-gap was inferred. The analysis of both quantities suggest that the gap decreases as the Ca-concentration grows (see Fig.31). Qualitatively similar results were found using polycrystals by Tsuji et al. (1996).

ii) In particular, for  $x=11.5$  and ambient pressure the gap was found to be finite and approximately 300K (actually from Knight shift the result is 270K, while from  $1/T_1$  it is 350K). This is important since at this Ca-concentration superconductivity has been observed upon the application of pressure by Nagata et al. (1997). Fig.32 shows the overall phase diagram obtained using NMR techniques. Note that the spin-gap seems to flatten as  $x$  continues growing, and it becomes unclear at what Ca-composition the gap will finally vanish if at all. The flattening of the spin-gap with Ca-composition is actually in contradiction with the previous results by Kumagai et al. (1997) using polycrystals. Note that in spite of the presence of a nearly constant spin-gap at large  $x$ , the conductivity changes substantially with increasing Ca-concentration.

iii) From data corresponding to  $T_{2G}$ , the spin correlation length  $\xi$  was obtained experimentally. It was found to decrease as  $x$  grows, as expected. Assuming this length is dominated by the mean distance among mobile holes, at Ca11.5 a hole concentration of  $x=0.25$  holes per  $\text{Cu}_2\text{O}_3$  was obtained. This value is in good agreement with the hole concentration  $x=0.22$  inferred from optical measurements by Osafune et al. (1997).

iv) At a temperature of around 60K, charge localization takes place. The resistivity increases in this regime.

v) The resistivity has a very interesting behavior with temperature as already discussed elsewhere in this review. At “high” temperatures the resistivity along the  $c$ -axis (i.e. along the legs of the ladders) is linear, while in the perpendicular direction the resistivity is  $T$ -independent and larger by an order of magnitude. The spin dynamics was found to be consistent with the  $S=1/2$  1D Heisenberg model. In an intermediate temperature regime the resistivity deviates slightly from the linear  $T$ -dependence, again similarly as it occurs in the 2D doped cuprates in the pseudogap region, while  $\rho_a$  grows as  $T$

decreases. These results suggest that in this regime pairs are expected to be formed, but they are confined into the ladders. In the “low” temperature regime, charge localization takes place presumably through the localization of the hole pairs on the ladders. In order to understand whether the application of pressure deconfines the hole pairs from the ladders, NMR studies should be carried out in the regime of high pressure and some results are already available as discussed below.

Several other NMR experiments on ladder materials have also been reported. They include Cu-NQR measurements for  $\text{Sr}_{14}\text{Cu}_{24}\text{O}_{41}$  by Carretta, Vietkin, and Revcolevschi (1998), and  $^{17}\text{O}$  NMR in doped and undoped  $\text{A}_{14}\text{Cu}_{24}\text{O}_{41}$  ( $\text{A}_{14} = \text{La}_6\text{Ca}_8, \text{Sr}_{11}\text{Ca}_3$ ) by Imai et al. (1998). A comprehensive  $^{63,65}\text{Cu}$  NMR/NQR study by Takigawa et al. (1998) on single crystals of undoped 14-24-41 reported two distinct resonance spectra for the chains, assigned to magnetic Cu-sites and nonmagnetic Zhang-Rice singlets. Microwave frequencies studies of the dynamical magnetic susceptibility by Zhai et al. (1999) show indications of charge ordering in the doped 14-24-41 material.

More recently, Mayaffre et al. (1998) reported  $^{63}\text{Cu}$  NMR measurements of the Knight shift and relaxation time  $T_1$  on the  $x=12$  Ca-doped 14-24-41 compound at high pressure. When the system becomes superconducting at 5K and 31 kilobars, those authors argued that the spin-gap collapsed based on, e.g., the relaxation rate  $T_1^{-1}$  vs temperature data shown in Fig.33. In addition, since they observe that superconductivity starts when the ladder spin-gap collapses, they argue that the ladder is responsible for the superconducting phase. It may occur that the preformed pairs on the two-leg ladders become dissociated upon pressure, making possible the hole hopping in the direction perpendicular to the legs. Regarding this interesting NMR data by Mayaffre et al. (1998), this author believes that it is important to obtain an independent confirmation of such an important result. Very recently, Mito et al. (1998) using once again NMR techniques at high pressure for a single crystal of 14-24-41 with  $x=12$  studied the Knight shift and  $T_1$  vs temperature up to pressures 1.7 GPa. They found a robust spin gap in their studies of magnitude quite similar to the result obtained at ambient pressure. It is difficult to understand how this gap can disappear so abruptly as the pressure goes up to 3 GPa, as claimed by Mayaffre et al. (1998). Hopefully Mito et al. will be able to extend their analysis to higher pressures in the near future. In addition, it should be investigated to what extent the collapse of the spin-gap reported by Mayaffre et al. (1998) corresponds to the creation of a small population of low-energy excitations by pressure, leaving large weight at the original spin-gap position which may remain mostly untouched as a high-energy feature, similarly as it has been shown theoretically to occur in the  $t$ - $J$  model for two-leg ladders doped with vacancies by Martins et al. (1996,1997). In other words, it would be interesting to investigate if the results of Mayaffre et al.

(1998) correspond to the replacement of a hard-gap by a “pseudogap”, namely a clear depletion in the spin density of states at low-energy which, however, does not vanish at any finite energy. Such a behavior is known to occur in the high temperature superconductors, and it would be very important to analyze to what extent doped ladders present a similar pseudogap phenomenology. Actually very recent NMR experiments by Auban-Senzier et al. (1999) already support the conjecture discussed here that a pseudogap appears in doped ladders at the high pressures needed to reach the superconducting state.

### 3.3.5 Inelastic Neutron Scattering:

Inelastic neutron scattering (INS) experiments on the 14-24-41 compound have also been reported. Using this technique, Eccleston, Azuma and Takano (1996) analyzed a polycrystalline sample of  $x=2.8$  14-24-41 and they observed a gap of 35 meV for the ladder. Broad features at 10 meV corresponding to chain excitations were also reported. More recently, Eccleston et al. (1998) presented the first INS study which has been able to access the spin ladder excitations using single crystals of a cuprate ladder material. A ladder spin-gap of  $32.5 \pm 0.1$  meV was reported with the scattering function  $S(\mathbf{q}, \omega)$  sharply peaked about the antiferromagnetic zone center. A band maximum at  $193.5 \pm 2.4$  meV was also observed. Excitations at energy transfers of 15 meV or below were assigned to the chains present in 14-24-41. INS results with emphasis on the physics of chains have also been reported recently by Regnault et al. (1998) and Matsuda et al. (1998), adding to the studies of Hiroi et al. (1996), Matsuda et al. (1996), Matsuda et al. (1997), D. E. Cox et al. (1998), and others that have concentrated their efforts on the analysis of that portion of the structure of 14-24-41. The rich physics of dimerized chains observed in this compound will not be reviewed here since the focus of the paper is on the physics of ladders, but it is clear that its analysis deserves further attention.

Recent inelastic neutron scattering results by Katano et al. (1999) for single crystal of  $x=11.5$  14-24-41 at both ambient pressure and high pressure of 0.72, 2.1 and 3.0 GPa produced surprising conclusions. Contrary to the NMR results of Magishi et al. (1998), Katano et al. (1999) reported a spin-gap in the doped system which does *not* change from that of the parent material. This occurs even under high pressure. The origin of these differences between NMR and INS is unclear at present (see Fig.34). Note that for  $x=11.5$  in the 14-24-41 material superconductivity appears between 3.5 GPa and 8 GPa, i.e. very close in pressure to where the last set of experiments by Katano et al. (1999) have been carried out. Note also that the INS data, if valid at slightly larger densities, would be in contradiction with the results of Mayaffre et al. (1998) that reported the absence of a spin-gap in the  $x=12$  14-24-41 compound under 3.2 GPa of pressure. This author would like to remark that

the analysis of the pressure dependence of the INS data into the pressure range of the superconducting state is very important, it should certainly continue, and further work hopefully will solve the discrepancy between INS and NMR results.

### 3.3.6 Photoemission and Angle-Resolved Photoemission $A(\mathbf{p}, \omega)$ :

Angle-resolved photoemission studies of the ladder compound  $\text{Sr}_{14-x}\text{Ca}_x\text{Cu}_{24}\text{O}_{41}$  have been carried out by Takahashi et al. (1997) and Sato et al. (1997) using single crystals with  $x=0$  and 9. These authors found two dispersive features in their data. One has an energy dispersion of about 0.5 eV, matching well the periodicity of the ladder. The minimum binding energy is located at momentum  $ka = \pi/2$  for  $x=0$ , in rough agreement with numerical studies of the t-J model by Tsunetsugu, Troyer and Rice (1994,1995); Troyer, Tsunetsugu, and Rice (1996); Haas and Dagotto (1996); and Martins, Gazza, and Dagotto (1999), that locate this minimum close to, although not exactly at,  $\pi/2$  in the bonding band of isolated ladders. The other features in the photoemission results by Takahashi et al. (1997) are deeper in energy, and they seem to correspond to chain excitations.

Other studies of the electronic structure of  $(\text{La}, \text{Sr}, \text{Ca})_{14}\text{Cu}_{24}\text{O}_{41}$  using core-level photoemission spectroscopy have been presented by Mizokawa et al. (1998), and the results compared against another ladder compound,  $\text{La}_{1-x}\text{Sr}_x\text{CuO}_{2.5}$ , as well as the high- $T_c$  material  $\text{La}_{2-x}\text{Sr}_x\text{CuO}_4$ . These authors observed that the chemical potential shift in doped 14-24-41 is considerably suppressed compared with the other two compounds, as shown in Fig.35. Mizokawa et al. (1998) interpreted this as an indication of a non-Fermi liquid state on the 14-24-41 ladders being more robust against hole doping than in other copper oxides.

This interesting result shows that much remains to be learned about ladders using photoemission experiments and hopefully in the future information as rich as reported for the high- $T_c$  compounds will be also available for ladders. In this context theory is still ahead of experiments and a considerable amount of information is already available to contrast experiments with results for the t-J model (see for instance Riera, Poilblanc and Dagotto, 1999). In particular, Martins et al. (1999) using a novel technique that allowed them to study clusters containing  $2 \times 20$  sites recently reported the evolution with doping of the dominant peak in the one-particle spectral function  $A(\mathbf{q}, \omega)$ , presumed to be a quasiparticle, as a function of density. The result is shown in Fig.36 for the bonding band  $q_y = 0$ . At  $x=0.0$  (undoped limit) the bonding band is very narrow. At  $x=0.125$ , it remains flat near  $(\pi, 0)$  quite similarly as in experiments for the 2D cuprates. A gap develops at this density due to pair formation. As  $x$  keeps on growing the photoemission

and inverse-photoemission bands lose their flatness, and start deforming resembling more a quasi-non-interacting dispersion which is reached at  $x=0.5$ . This theoretical result is the first one available where the evolution of the one-particle spectral function with doping has been reported between a limit dominated by short-range antiferromagnetic correlations and a quasi-non-interacting regime. The analog result for the 2D cuprates is still unknown.

### 3.4 The Strong-Coupling Ladder Compound $\text{Cu}_2(\text{C}_5\text{H}_{12}\text{N}_2)_2\text{Cl}_4$

Spin ladders belonging to the organic family of materials have also been synthesized. In particular, the compound  $\text{Cu}_2(\text{C}_5\text{H}_{12}\text{N}_2)_2\text{Cl}_4$  has Cu-ions which are coupled antiferromagnetically in isolated ladders, as remarked by Chaboussant et al. (1997a,1997b). The schematic structure of this compound is shown in Fig.37. The coupling between coppers is mediated by chlorine ions (not shown in Fig.37). The orbitals involved in the process have a small overlap producing a reduced value for that coupling. Experimentally, the Heisenberg exchanges were found to be  $J_{\perp} = 13.2\text{K}$  and  $J_{\parallel} = 2.4\text{K}$ , following the notation of Fig.37, leading to an anisotropic ladder that belongs to the strong coupling limit since  $J_{\perp}/J_{\parallel} = 5.5$  (Chaboussant et al., 1997b). In this case, the rung spin-singlet must be very strong, leading to a regime which is under good control in the theoretical calculations using t-J-like models. The physics in this strong coupling region of parameter space is expected to be smoothly connected to the isotropic regime  $J_{\perp} \sim J_{\parallel}$ , as discussed in Sec.2 and by Dagotto, Riera and Scalapino (1992). In addition, the intrinsic small values of the Heisenberg couplings allows for investigations in static magnetic fields of comparable strength, providing a window of research that is not possible in the inorganic cuprate ladders with exchange couplings of order  $0.1\text{eV} \sim 1000\text{K}$ . Since at large  $J_{\perp}/J_{\parallel}$  the dominant spin configurations are singlets along the rungs, the lowest-energy excitations correspond to local rung-triplets which can move along the ladder. A finite density of these excitations is needed to represent the physics of ladders in high magnetic fields of strength large enough to produce a finite magnetization.

After NMR techniques were applied to the organic ladder compound by Chaboussant et al. (1997b), a spin gap  $\Delta \sim J_{\perp} - J_{\parallel}$  was reported, in agreement with theoretical expectations at large  $J_{\perp}/J_{\parallel}$ . In addition, the gap obtained from the static susceptibility  $\chi$  and the dynamical spin structure factor obtained from the NMR measurements were found to be identical, as predicted by theory. Further work by Chaboussant et al. (1998a), still using NMR methods, analyzed the transition from the gapped spin-liquid state to a gapless magnetic regime. At the critical magnetic field  $H_{c1} \sim 7.5\text{T}$  where the gap closes, the system is in a quantum critical regime where the temperature is the only relevant scale. At

a larger field,  $H_{c2}$ , the system becomes fully polarized. Measurements of the susceptibility and magnetization in this regime are in good agreement with calculations by Weihong, Singh, and Oitmaa (1997) (see also Hayward, Poilblanc and Levy (1996)). More recent studies of the organic ladder by Calemczuk et al. (1999), based on specific heat data, reported a possible incommensurate gapped state due to a small magneto-elastic coupling of the isolated ladders with the 3D lattice. Associating the rung-singlet and rung-triplet states, the latter having spin projection along the magnetic field, with fictitious “spin” states up and down, Chaboussant et al. (1998b) argued that the physics of strongly coupled ladders in high magnetic fields can be mapped into a 1D XXZ Heisenberg spin model which is known from previous investigations to present incommensurate phases in magnetic fields. Calculating the magnetization with the Bethe Ansatz applied to the XXZ model and comparing the results with the experimental magnetization leads to an excellent agreement (see Fig.38). Since the XXZ model is equivalent to spinless fermions which in 1D form Luttinger liquid (LL) states, a regime with these characteristics was conjectured to exist between  $H_{c1}$  and  $H_{c2}$ , as indicated in Fig.39. At very low temperatures the small couplings between ladders will destabilize the LL leading to a charge ordered state, as also sketched in Fig.39.

Other recent developments in this context include the presence of plateaux in the magnetization curve in the vicinity of  $(H_{c1} + H_{c2})/2$ , as argued by Cabra, Honecker and Pujol (1997), Cabra and Grynberg (1998) and others. Calculations for coupled ladders in a magnetic field have also been recently reported by Giamarchi and Tsvelik (1998). Other studies in magnetic fields were presented by Schmeltzer and Bishop (1998). In addition, some of the results derived in terms of a ladder with only two couplings ( $J_{\perp}, J_{\parallel}$ ) are controversial since Hammar et al. (1998) argued that extra ladder couplings, as well as multimagnon excitations and interladder couplings, may be needed to properly reproduce their inelastic neutron scattering and specific heat data (see also Hayward, Poilblanc, and Levy (1996)). Overall it is clear that the analysis of ladder systems under high magnetic fields have already revealed an unexpected rich structure, and theoretical and experimental efforts should continue exploring this interesting regime in parameter space.

Finally, doping with impurities the organic ladder can reveal interesting physics. Using computational techniques, Laukamp et al. (1998) predicted that Zn-doping of the organic strong-coupling ladder should not produce important changes in the spin-gap, contrary to what is observed in other Zn-doped ladders. Experiments are already in agreement with this prediction (see Deguchi et al. (1998)).

### 3.5 Vanadium-based Ladder Compound $\text{CaV}_2\text{O}_5$

Interesting studies by Iwase et al. (1996) showed that the vanadate  $\text{CaV}_2\text{O}_5$  has a large spin-gap of about 500K. The structure of this compound corresponds to a depleted two-dimensional square lattice. It consists of a so-called trellis-lattice with two-leg ladders containing V-ions in a  $V^{4+}$  state of spin-1/2, with the idealized structure shown in Fig.40. The ladders are coupled through  $90^\circ$  oxygen bonds which are expected to produce a weak exchange, geometry similar as in some of the cuprate ladder materials, although involving the vanadium  $d_{xy}$ -orbitals. Actually, studies by Normand et al. (1997) reported couplings  $J_\perp/J_\parallel \sim 4.3$  and  $J_\parallel/J' \sim 3.5$ , in the notation of Fig.40. However, recent Quantum Monte Carlo simulations of the trellis-lattice Heisenberg model by Miyahara et al. (1998) produced a magnetic susceptibility vs temperature in agreement with experiments if  $J_\perp \sim 670\text{K}$ ,  $J_\parallel \sim 67\text{K}$ , and  $J' \sim 45\text{K}$ , namely using  $J_\parallel \sim J'$ . This result suggests that the dominant structures in the vanadate ladders are the dimers or rungs with spins coupled by  $J_\perp$ , rather than the ladders themselves. The resolution of this discrepancy is important to decide whether  $\text{CaV}_2\text{O}_5$  should be considered as a two-leg ladder material.

More recently, the compound  $\text{MgV}_2\text{O}_5$  has also been studied (see Millet et al., 1998). The V-oxide planes of this material are very similar to those of  $\text{CaV}_2\text{O}_5$ . However, the observed gap is just 15K, much smaller than the 500K reported for the latter. The difference was explained by Millet et al. (1998) on the basis of a frustrated coupled ladder model. Other recent developments involve the spin-Peierls compound  $\text{NaV}_2\text{O}_5$ . Based on the determination of the crystal structure of this compound by x-ray diffraction and on density-functional calculations, Smolinski et al. (1998) argued that  $\text{NaV}_2\text{O}_5$  can be considered a quarter-filled two-leg ladder system. The exchange interaction of  $\text{NaV}_2\text{O}_5$  across the rungs was found to be larger than along the legs by a factor 5. Since this compound and  $\text{CaV}_2\text{O}_5$  are isostructural, it was also argued that the latter should also be regarded as a (half-filled) ladder system instead of only having isolated dimers (see discussion in previous paragraph). Very recent results by Lemmens et al. (1998) using Raman scattering applied to  $\text{NaV}_2\text{O}_5$  showed an interesting sequence of magnetic bound states at low temperatures. The importance of doping  $\text{NaV}_2\text{O}_5$  away from quarter-filling was remarked by Smolinski et al. (1998). Clearly this system provides a new playground to test the interplay between spin, charge, orbital and lattice degrees of freedom in a ladder geometry, and further work should be pursued in this context.

### 3.6 The Ladder Compound $\text{KCuCl}_3$

Recently, Tanaka et al. (1996) have presented interesting arguments suggesting that the material  $\text{KCuCl}_3$  can also be described as a double spin-chain system. The crystal structure of this compound is shown in Fig.41.

The main feature is the double chain of edge-sharing  $\text{CuCl}_6$  octahedra along the  $a$ -axis. Also in Fig.41 it is shown the expected pattern of Heisenberg exchange couplings arising from such a structure. They involve not only the standard rung- and leg-couplings, but also a plaquette-diagonal coupling. Their values are expected to be small since  $\sim 90^\circ$  bonds are involved in the structure. To investigate the nature of the ground state of this material, Tanaka et al. (1996) studied the temperature dependence of the magnetic susceptibility. The low-temperature results can be fit very well with the formula  $\chi \sim (1/\sqrt{T})\exp(-\Delta/k_B T)$  proposed by Troyer, Tsunetsugu and Würtz (1994). The gap obtained by this procedure was found to be 35K. Large scale quantum Monte Carlo calculations performed by Nakamura and Okamoto (1998) on the spin model believed to describe this material, found an agreement with the experimental data within 1% relative errors in the full range of temperatures investigated. The comparison theory-experiment involved neutrons scattering data obtained by Kato et al. (1998). The couplings that reproduce the experimental data the best are  $J_1 = 12.3\text{K}$ ,  $J_2 = 4J_1$ , and  $J_3 \sim 0$  suggesting that the extra coupling  $J_3$  may not be necessary. In addition, note that related double-spin chain systems, such as  $\text{NH}_4\text{CuCl}_3$ , have also been studied using ESR and other techniques by Takatsu et al. (1997) and Kurniawan et al. (1999).

The values of the exchange couplings that have been reported for  $\text{KCuCl}_3$  locate the material in the strong rung-coupling limit, similarly as it occurs for the  $\text{Cu}_2(\text{C}_5\text{H}_{12}\text{N}_2)_2\text{Cl}_4$  compound, as explained before in this review. For this reason it is natural for this author to suggest the use of (probably pulsed) high magnetic fields for the study of  $H_{c1}$ , which is the magnetic field at which the gapped spin state becomes gapless (for results with high fields see Shiramura et al. (1997)). The motivation is to investigate whether the interesting physics reported by Chaboussant et al. (1998b) is also present in  $\text{KCuCl}_3$ , especially regarding the possible presence of incommensurate spin correlations. Also the chemical replacement of Cu-ions by Zn- or Ni-ions would add to the ongoing discussion on the influence of vacancies on the physics of ladders and spin-Peierls systems, as discussed earlier in the paper (see Martins et al., 1997, and references therein. See also Sandvik, Dagotto and Scalapino, 1997).

## IV. CONCLUSIONS

In this review the experimental aspects of the study of ladder materials have been discussed, with emphasis on the relation with the high- $T_c$  cuprates and contrasting the results with theoretical predictions. After a considerable effort, a variety of experiments have clearly confirmed the predicted existence of a spin-gap in two-leg ladders, a feature that in the form of a pseudogap also

appears in the underdoped 2D cuprates. This is an important achievement of theoretical calculations, showing that at least in spin systems and low-dimensions the models and many-body tools available are powerful enough to make reliable predictions. Even in the context of Zn-doped ladders a good agreement theory-experiments has been reported. Here small amounts of vacancies produce a considerable enhancement of the antiferromagnetic correlations in their vicinity and the ladders develop long-range order out of an apparently disordering procedure. Some other undoped ladders are in the strong rung-coupling regime and the values of their couplings are such that they can be studied in high magnetic fields, leading to a rich phase diagram that is also in good agreement with theoretical studies. Overall, the analysis of ladders in the absence of mobile holes seems under good control.

Once carriers are added to some of the available ladder compounds, a metal-insulator transition has been observed. At ambient pressure the carriers seem confined to move along the ladders. As the pressure increases, the hole movement along the rung direction is enhanced and superconductivity appears in the 14-24-41 ladder. Pressure is presumed to increase the interladder couplings. Actually it has become clear that such couplings are not negligible in several real ladders even in the undoped regime, causing transitions to antiferromagnetic states at low temperatures. While most authors agree with the notion that hole pairs are created on the ladders, probably by the mechanism predicted by the theorists, it is still under discussion what triggers the transition to the superconducting phase. It may occur that the interladder hopping is important to prevent the system from forming a charge-density-wave of pairs, that some experiments have detected at low-pressure. In this respect a large pressure is needed to provide extra mobility to the carriers, but too much pressure would conspire against the formation of pairs on the individual ladders. This may explain the existence of an optimal pressure. In addition, theoretical studies have shown that in the undoped regime an apparently small interladder coupling may destroy the spin-gap and transform the ground state into a gapless antiferromagnet. Since the presence of spin-gap features is important for the superconductivity predicted by the theorists, once again it is concluded that too much pressure may be detrimental for superconductivity.

Some experimental aspects are still controversial, notably the value of the spin-gap as the hole concentration and pressure changes in 14-24-41. Some NMR experiments associate the closing of the spin-gap with the appearance of superconductivity. However, other NMR and neutron scattering experiments at slightly smaller pressures report a very robust spin-gap. Hopefully these differences will be clarified in the near future. Resistivity measurements for this compound have found that the system becomes metallic both along the leg and rung directions at the optimal pressure. Similarities of this behavior with results for two-dimensional cuprates have been here remarked by the author. A possible underdoped-

like regime could exist in 14-24-41 in a narrow pressure window. Note that regardless of the 1D vs 2D character of the superconductivity, x-ray experiments have confirmed the survival of the ladder substructures in the 14-24-41 material under high pressure. Then, this compound is the *first* copper-oxide superconductor with a non-square-lattice arrangement. In addition, the resistivity versus temperature on the 14-24-41 ladder is linear at several concentrations adding to the list of common aspects with the 2D cuprates. Several other similarities have been discussed in the paper. Certainly much can be learned out of a superconducting compound that has the same Cu and O building blocks as the high- $T_c$  materials.

The overall conclusion is that the analysis of ladder compounds has already developed into a fruitful area of research, and quite challenging and interesting results have become available in recent years. Among the most notable discoveries are a novel copper-oxide superconducting material with a ladder-dominated structure, and several others compounds with a clear spin-gap in their spectrum. Further work in the context of ladders will likely keep on providing key information to unveil the mystery of the origin of superconductivity in the cuprates and the behavior of electrons in transition-metal-oxides in general.

## V. ACKNOWLEDGMENTS

Part of the results discussed here have emerged from conversations and discussions with several colleagues working on ladder compounds. The author especially thanks J. Akimitsu, M. Azuma, T. Barnes, G. Chaboussant, L. Degiorgi, A. Fujimori, Z. Hiroi, D. Jérôme, D. C. Johnston, M-H. Julien, Y. Kitaoka, A. Moreo, D. Poilblanc, T. M. Rice, J. Riera, D. J. Scalapino, M. Takano, S. Uchida, for their comments. The author is supported in part by grant NSF-DMR-9814350.



## FIGURE CAPTIONS

1. (a) Schematic representation of the ground state of a two-leg ladder. Pairs of spins along the same rung tend to form a spin singlet; (b) Individual holes added to the ladders destroy spin singlets; (c) To minimize the energy damage caused by the addition of holes, these holes tend to share the same rung forming hole bound-states. Figure reproduced from Hiroi (1996).
2. Spin-gap  $\Delta_{\text{spin}}$  versus the ratio  $J'/J$  for the two-leg ladder, with the convention that  $J'$  is the coupling along the rungs and  $J$  along the legs. The results are extrapolations to the bulk limit of data obtained on finite  $2 \times N$  clusters. The figure is reproduced from Barnes et al. (1993).
3. Susceptibility as a function of temperature for the single chain and the Heisenberg ladders with up to six legs, obtained by Frischmuth, Ammon and Troyer (1996) using a Monte Carlo algorithm. The upper and lower parts of the figure differ in the temperature range analyzed. At low-temperature, frame (b) clearly shows that the odd- and even-leg ladders have a qualitatively different behavior, as described in the text.
4. Log-log plot of various correlation functions versus the real space separation  $|i - j|$  for a  $2 \times 30$  open chain with density  $\langle n \rangle = 0.8$  and  $J/t = 1.0$ . The dashed line has a slope -2 and the dotted line -1. Figure taken from Hayward et al. (1995), where more details can be found on the definition of the correlation functions used here.
5. Dynamical spin structure factor  $S(\mathbf{q}, \omega)$  for the  $q_y = \pi$  branch of a  $2 \times 16$  cluster with two holes. The physical meaning of branches (I) and (II) is explained in the text. The figure is taken from Dagotto et al. (1998) using a technique involving a small fraction of the Hilbert space, after the t-J model is rewritten (exactly) in the rung-basis.
6. Schematic representation of (a) the  $\text{Cu}_2\text{O}_3$  sheets of  $\text{SrCu}_2\text{O}_3$  (from Azuma et al., 1994). The three-leg ladder  $\text{Sr}_2\text{Cu}_3\text{O}_5$  is also shown in (b). The filled circles are  $\text{Cu}^{2+}$  ions, and  $\text{O}^{2-}$  ions are located at the corners of the squares drawn with solid lines.
7. Temperature dependence of the magnetic susceptibility of  $\text{SrCu}_2\text{O}_3$  (from Azuma et al., 1994). Details can be found in the text.
8. Similar as Fig. 7 but for the three-leg compound  $\text{Sr}_2\text{Cu}_3\text{O}_5$  (from Azuma et al., 1994). In this case a large susceptibility is observed even at low temperatures, indicative of the absence of a spin-gap, in agreement with theoretical expectations.
9. Magnetic susceptibility vs temperature for  $\text{SrCu}_2\text{O}_3$  (filled circles). Shown as open symbols are fits to these data using the calculations of Barnes and Riera (1994) for the isolated spin-1/2 two-leg ladder at several ratios of the rung Heisenberg coupling, here denoted by  $J'$ , and the leg coupling  $J$ . Figure reproduced from Johnston (1996). A comprehensive experimental paper with updated information about these issues is in preparation (D. Johnston, private communication).
10. Magnetic susceptibility of  $\text{Sr}(\text{Cu}_{1-x}\text{Zn}_x)_2\text{O}_3$  vs. temperature at several Zn-concentrations. The inset shows the temperature dependence of the inverse susceptibility. The results are reproduced from Azuma et al. (1997).
11. Local staggered susceptibility  $\chi_r(-1)^r$  along the upper leg of a  $2 \times 50$  ladder obtained with computational techniques (from Laukamp et al., 1998). Two vacancies are included in the system, located at rung 8 on the upper leg and 43 on the lower leg. Results for three values of the ratio  $J_{\text{rung}} = J_{\perp}/J$  are shown. For details see Laukamp et al. (1998).
12. Structure of  $\text{LaCuO}_{2.5}$  along the  $c$ -axis. Large, medium, and small balls represent La, Cu, and O atoms, respectively. The figure is reproduced from Hiroi (1996).
13. Temperature dependence of the magnetic susceptibility for  $\text{LaCuO}_{2.5}$ , from Hiroi (1996). The open circles are the raw data. The solid line through them is a fit including a temperature independent term, a Curie term due to impurities, plus the bulk susceptibility expected from a 2-leg Heisenberg ladder. The dotted line is the susceptibility after subtracting the Curie component. The other solid line corresponds to  $\text{SrCu}_2\text{O}_3$ , for comparison.
14. Resistivity of  $\text{La}_{1-x}\text{Sr}_x\text{CuO}_{2.5}$  vs. temperature for several Sr-compositions (reproduced from Hiroi, 1996).
15. Resistivity at 300K of  $\text{La}_{1-x}\text{Sr}_x\text{CuO}_{2.5}$  and  $\text{La}_{2-x}\text{Sr}_x\text{CuO}_4$ , and its doping dependence (reproduced from Hiroi, 1996).
16. Doping dependence of the magnetic susceptibility at several hole concentrations (from Hiroi, 1996).
17. (a) Crystal structure of  $(\text{Sr}, \text{Ca})_{14}\text{Cu}_{24}\text{O}_{41}$ . (b) and (c) show the  $\text{CuO}_2$  chain and  $\text{Cu}_2\text{O}_3$  ladder subunit, respectively. Figure reproduced from Magishi et al. (1998).
18. Electrical resistivity  $\rho$  of  $\text{Sr}_{0.4}\text{Ca}_{13.6}\text{Cu}_{24}\text{O}_{41.84}$  vs temperature below 50K, and under pressure of 3, 4.5 and 6 GPa, showing the existence of superconductivity. The figure is reproduced from Uehara et al. (1996).

19. Temperature dependence of the electrical resistivities at various pressures, for  $\text{Sr}_{0.4}\text{Ca}_{13.6}\text{Cu}_{24}\text{O}_{41+\delta}$ . Data reproduced from Isobe et al. (1998).
20. Temperature dependence of  $T_c$  (onset) as a function of pressure for  $\text{Sr}_{0.4}\text{Ca}_{13.6}\text{Cu}_{24}\text{O}_{41+\delta}$ , reproduced from Isobe et al. (1998).
21. Pressure variation of the lattice constants of  $\text{Sr}_{0.4}\text{Ca}_{13.6}\text{Cu}_{24}\text{O}_{41+\delta}$  at low temperature, reproduced from Isobe et al. (1998). The  $c$ -direction runs along the legs of the ladders,  $a$  along its rungs, and  $b$  is perpendicular to both.
22. Effect of pressure on the temperature dependence of the resistivity (a) along the leg-ladder direction ( $\rho_c$ ) and (b) across the rung-ladder direction ( $\rho_a$ ) of single crystal  $\text{Sr}_{2.5}\text{Ca}_{11.5}\text{Cu}_{24}\text{O}_{41}$  at the indicated pressures. The inset shows the pressure dependence of  $T_c$ . Figure reproduced from Nagata et al. (1998a).
23. Effect of pressure on the temperature dependence of the anisotropic ratio  $\rho_a/\rho_c$  of single crystal  $\text{Sr}_{2.5}\text{Ca}_{11.5}\text{Cu}_{24}\text{O}_{41}$  at the indicated pressures. The inset shows the same anisotropic ratio but at pressures above 4.5 GPa. Figure reproduced from Nagata et al. (1998a).
24. In-plane ( $\rho_a$ ) and out-of-plane ( $\rho_c$ ) resistivity of  $\text{YBa}_2\text{Cu}_3\text{O}_{7-y}$  plotted as a function of temperature, reproduced from Takenaka et al. (1994). Results are shown for various oxygen concentrations  $7-y \sim 6.68, 6.78, 6.88, \text{ and } 6.93$ .
25. Anisotropic resistivity ratio  $\rho_c/\rho_a$  plotted as a function of temperature for various oxygen contents (from Takenaka et al., 1994).
26.  $c$ -axis optical conductivity  $\sigma_c(\omega)$  of  $\text{Sr}_{14-x}\text{A}_x\text{Cu}_{24}\text{O}_{41}$  for various compositions. The figure is reproduced from Osafune et al. (1997). The anisotropic spectra with  $a$ - and  $c$ -axis polarization are shown for  $\text{Sr}_3\text{Ca}_{11}\text{Cu}_{24}\text{O}_{41}$  in the inset.
27. Effective electron number  $N_{\text{eff}}$  per Cu (left-hand scale) presented as a function of energy for various compositions. The valences of both chain- and ladder-Cu estimated for each composition are plotted in the inset. Details can be found in Osafune et al. (1997).
28. T-dependence of the resistivities along the legs ( $\rho_c$ ) and rungs ( $\rho_a$ ) of the ladders in the compound  $\text{Sr}_{14-x}\text{Ca}_x\text{Cu}_{24}\text{O}_{41}$ , with  $x=8$  and  $11$  (from Osafune et al, 1999). The temperatures  $T^*$  and  $T_0$  where  $d\rho/dT$  changes sign are indicated for  $x=11$ . The anisotropic resistivity  $\rho_a/\rho_c$  vs temperature is plotted in the inset.
29.  $a$ -axis optical conductivity spectra  $\sigma_a(\omega)$  below  $2500 \text{ cm}^{-1}$  at various temperatures are shown for  $x=8$  (upper panel) and  $11$  (lower panel) (from Osafune et al., 1999). In the inset are shown the spectra below  $800 \text{ cm}^{-1}$  to show the redistribution of the oscillator strength of the phonons.
30.  $c$ -axis optical conductivity spectra  $\sigma_c(\omega)$  at various temperatures for  $x=8$  (upper panel) and  $11$  (lower panel). The optical reflectivity spectra in the low frequency region are shown in each inset. This figure is from Osafune et al. (1999), which should be consulted for further details.
31.  $(1/T_1)_b$  for a magnetic field parallel to the  $b$ -axis vs  $1/T$ . Results are shown for several Ca-compositions of  $\text{Sr}_{14-x}\text{Ca}_x\text{Cu}_{24}\text{O}_{41}$ . The solid lines are fits to  $1/T_1 \sim \exp(-\Delta/T)$ . The inset contains the relaxation function of the nuclear magnetization at  $T=110\text{K}$  in  $\text{Ca}_{11.5}$ . The figure is reproduced from Magishi et al. (1998).
32. Spin gap vs the amount of Ca-substitution in  $\text{Sr}_{14-x}\text{Ca}_x\text{Cu}_{24}\text{O}_{41}$ , reproduced from Magishi et al. (1998). Also shown is  $T_c$  vs pressure at  $x=11.5$ . The spin gaps  $\Delta_K$  and  $\Delta_{T_1}$  are obtained from the Knight shift and  $T_1$ , respectively.  $T_L$  is the temperature associated with the localization of pairs. For more details see Magishi et al. (1998).
33. Temperature dependence of the  $^{63}\text{Cu}$  ladder relaxation rate  $T_1^{-1}$  at 1 bar and 32.2 kbar. Figure reproduced from Mayaffre et al. (1998).
34. Spin-gap as a function of Ca-content in [14,24,41] at ambient pressure. The circles show the results from neutron scattering experiments (Katano et al. (1999)). The triangles are the results from the Knight shift in the NMR experiments of Magishi et al. (1998). The figures is reproduced from Katano et al. (1999).
35. Chemical potential shift as a function of hole concentration of the Cu-O ladder for  $(\text{La}, \text{Sr}, \text{Ca})_{14}\text{Cu}_{24}\text{O}_{41}$  compared with that for  $(\text{La}, \text{Sr})\text{CuO}_{2.5}$ . These results are reproduced from Mizokawa et al. (1998). The hole concentration of the ladder has been taken from the optical study of Osafune et al. (1997).
36. Dominant peak in the one-particle spectral function  $A(\mathbf{p}, \omega)$  obtained numerically using the t-J model, parametric with hole density  $x$ . The coupling used was  $J/t=0.4$  and the lattice had up to  $2 \times 20$  sites. The size of the points is proportional to the intensity of the peak. Open circles correspond to photoemission, while full circles are in the inverse-photoemission region. Figure taken from Martins et al. (1999), where more details about the calculation can be found.

37. Schematic structure of  $\text{Cu}_2(\text{C}_5\text{H}_{12}\text{N}_2)_2\text{Cl}_4$ . The labeled protons contribute to the NMR lines study, as discussed by Chaboussant et al. (1997b).
38. Magnetization of  $\text{Cu}_2(\text{C}_5\text{H}_{12}\text{N}_2)_2\text{Cl}_4$  between 0 and 20 T, at different temperatures, reproduced from Chaboussant et al. (1998b). The symbols are experimental data points, while the solid lines are the fits to the XXZ model (for details, see the text and Chaboussant et al., 1998b). The critical fields are indicated.
39. Phase diagram of spin-ladders in a magnetic field, reproduced from Chaboussant et al. (1998b). The quantum critical regime at finite temperature above  $H_{c1}$  is shown. The “LL” label corresponds to a possible Luttinger liquid region. Further details can be found in Chaboussant et al. (1998b).
40. Schematic representation of the trellis-lattice corresponding to the structure of the vanadates, reproduced from Miyahara et al. (1998). The full circles are the positions of the V-ions. The oxygens in between are not shown. The couplings that are shown correspond to the Heisenberg exchange constants used to model the behavior of this material.
41. The double chain structure in  $\text{KCuCl}_3$  and the configuration of the hole orbital  $d(x^2 - y^2)$  of the  $\text{Cu}^{2+}$  ion are shown in the upper panel. Filled and open circles are  $\text{Cu}^{2+}$  and  $\text{Cl}^-$  ions, respectively. In the lower panel, the structure of the exchange interactions expected in the present system is shown. The figure is reproduced from Tanaka et al. (1996).

## REFERENCES

- Ando Y, Boebinger GS, Passner A, Kimura T and Kishio K 1995 Phys. Rev. Lett. **75** 4662-4665.
- Arai M and Tsunetsugu H 1997 Phys. Rev. **B 56**, R4305.
- Asai Y 1994 Phys. Rev. **B 50** 6519.
- Auban-Senzier P, Mayaffre H, Lefebvre S, Wzietek P, Jérôme D, Ammerahl U, Dhahenne G and Revcolevschi A 1999 preprint, to appear in Proceedings of the International Conference on Synthetic Metals 1998.
- Azuma M, Hiroi Z, Takano M, Ishida K and Kitaoka Y 1994 Phys. Rev. Lett. **73**, 3463.
- Azuma M, Fujishiro Y, Takano M, Nohara M and Takagi H 1997 Phys. Rev. **B 55**, R8658.
- Azzouz M, Chen L, and Moukouri S 1994 Phys. Rev. **B 50** 6233.
- Balakirev FF, Betts JB, Boebinger GS, Motoyama N, Eisaki H and Uchida S 1998 cond-mat/9808284.
- Balents L and Fisher MPA 1996a Phys. Rev. **B 53** 12133.
- Balents L and Fisher MPA 1996b cond-mat/9611126.
- Barnes T, Dagotto E, Riera J and Swanson E 1993 Phys. Rev. **B 47**, 3196.
- Barnes T and Riera J 1994 Phys. Rev. **B 50**, 6817.
- Bednorz JG and Müller KA 1986 Z. Phys. B **64** 188.
- Boebinger GS, Ando Y, Passner A, Kimura T, Okuya M, Shimoyama J, Kishio K, Tamasaku K, Ichikawa N and Uchida S 1996 Phys. Rev. Lett. **77** 5417-5420.
- Cabra D, Honecker A and Pujol P 1997 Phys. Rev. Lett. **79**, 5126.
- Cabra D and Grynberg M, preprint, cond-mat/9810263 and references therein.
- Calemczuk R, Riera J, Poilblanc D, Boucher JP, Chaboussant G, Levy L and Piovesana O 1999 Eur. Phys. J. B **7**, 171.
- Carretta P, Vietkin A and Revcolevschi A 1998 Phys. Rev. **B 57**, R5606.
- Carretta P, Ghigna P and Lascialfari A 1998 Phys. Rev. **B 57**, 11545.
- Carter SA, Batlogg B, Cava RJ, Krajewski JJ, Peck WF Jr and Rice TM 1996 Phys. Rev. Lett. **77**, 1378.
- Chaboussant G, Crowell PA, Levy LP, Piovesana O, Madouri A and Mailly D 1997a Phys. Rev. **B 55**, 3046.
- Chaboussant G, Julien M-H, Fagot-Revurat Y, Levy LP, Berthier C, Horvatic M and Piovesana O 1997b Phys. Rev. Lett. **79**, 925.
- Chaboussant G, Fagot-Revurat Y, Julien M-H, Hanson M, Berthier C, Horvatic M, Levy LP and Piovesana O 1998a Phys. Rev. Lett. **80**, 2713.
- Chaboussant G, Julien M-H, Fagot-Revurat Y, Hanson M, Levy LP, Berthier C, Horvatic M and Piovesana O 1998b Eur. Phys. J. B **6**, 167.
- Cox DE, Iglesias T, Hirota K, Shirane G, Matsuda M, Motoyama N, Eisaki H and Uchida S 1998 Phys. Rev. **B 57**, 10750.
- Dagotto E and Moreo A 1988 Phys. Rev. **B 38**, 5087
- Dagotto E, Riera J and Scalapino DJ 1992 Phys. Rev. **B 45**, 5744.
- Dagotto E 1994 Rev. Mod. Phys. **66** 763.
- Dagotto E and Rice TM 1996 Science **271**, 618.
- Dagotto E, Martins G, Riera J, Malvezzi A and Gazza C 1998 Phys. Rev. **B 58**, 12063.
- Deguchi H, Sumoto S, Takagi S, Mito M, Kawae T, Takeda K, Nojiri H, Sakon T and Motokawa M 1998 J. Phys. Soc. Jpn. **67**, 3707.
- Eccleston RS, Barnes T, Brody J and Johnson JW 1994 Phys. Rev. Lett. **73**, 2626.
- Eccleston RS, Azuma M and Takano M 1996 Phys. Rev. **B 53**, R14721.
- Eccleston RS, Uehara M, Akimitsu J, Eisaki H, Motoyama N and Uchida S 1998 Phys. Rev. Lett. **81** 1702-1705.
- Emery VJ, Kivelson SA and Zachar O 1997 Phys. Rev. **B 56**, 6120, and references therein.
- Emery VJ, Kivelson SA and Zachar O 1998 cond-mat/9810155.
- Frischmuth B, Ammon B and Troyer M 1996 Phys. Rev. **B 54** R3714.
- Fujiwara N, Yasuoka H, Fujishiro Y, Azuma M and Takano M 1998 Phys. Rev. Lett. **80**, 604.

- Fukuzumi Y, Mizuhashi K, Takenaka K and Uchida S 1996 Phys. Rev. Lett. **76**, 684.
- Garrett AW, Nagler SE, Tennant DA, Sales BC and Barnes T 1997a Phys. Rev. Lett. **79**, 745.
- Garrett AW, Nagler SE, Barnes T and Sales BC 1997b Phys. Rev. **B 55**, 3631.
- Gayen S and Bose I 1995 J. Phys. C **7** 5871.
- Gazza C, Martins G, Riera J and Dagotto E 1999 Phys. Rev. **B 59**, R709.
- Giamarchi T and Tsvelik AM 1998 cond-mat/9810219, and references therein.
- Gopalan S, Rice TM and Sigrist M 1994 Phys. Rev. **B 49**, 8901.
- Greven M, Birgeneau RJ and Wiese UJ 1996 Phys. Rev. Lett. **77** 1865.
- Greven M, Birgeneau R and Wiese UJ 1997 "Physics News in 1996", Supplement to the APS News, May 1997, page 12.
- Haas S and Dagotto E 1996 Phys. Rev. **B 54**, R3718.
- Hammar P, Reich D, Broholm C and Trouw F 1998 Phys. Rev. **B 57**, 7846.
- Hansen P, Riera J, Delia A and Dagotto E 1998 Phys. Rev. **B 58** 6258.
- Hayward CA, Poilblanc D, Noack RM, Scalapino DJ and Hanke W 1995 Phys. Rev. Lett. **75**, 926.
- Hayward CA, Poilblanc D and Scalapino DJ 1996 Phys. Rev. **B 53**, R8863.
- Hayward CA and Poilblanc D 1996 Phys. Rev. **B 53**, 11721.
- Hayward CA, Poilblanc D and Levy LP 1996 Phys. Rev. **B 54**, 12649.
- Hiroi Z, Azuma M, Takano M and Bando Y 1991 J. Solid State Chem. **95**, 230.
- Hiroi Z and Takano M 1995 Nature **377**, 41.
- Hiroi Z 1996 J. of Solid State Chem. **123**, 223.
- Hiroi Z, Amelinckx S, Van Tendeloo G and Kobayashi N 1996 Phys. Rev. **B 54**, 15849.
- Homes CC, Timusk T, Liang R, Bonn DA and Hardy WN 1993 Phys. Rev. Lett. **71**, 1645.
- Imai T, Thurber KR, Shen KM, Hunt AW and Chou FC 1998 Phys. Rev. Lett. **81** 220.
- Ishida K, Kitaoka Y, Asayama K, Azuma M, Hiroi Z and Takano M 1994 J. Phys. Soc. Jpn. **63**, 3222.
- Ishida K, Kitaoka Y, Tokunaga Y, Matsumoto S, Asayama K, Azuma M, Hiroi Z and Takano M 1996 Phys. Rev. **B 53**, 2827.
- Isobe M, Ohta T, Onoda M, Izumi F, Nakano S, Li J, Matsui Y, Takayama-Muromachi E, Matsumoto T and Hayakawa H 1998 Phys. Rev. **B 57**, 613.
- Iwase H, Isobe M, Ueda Y and Yasuoka H 1996 J. Phys. Soc. Jpn. **65** 2397.
- Johnston DC, Johnson JW, Goshorn DP and Jacobson AP 1987 Phys. Rev. **B 35** 219.
- Johnston DC 1996 Phys. Rev. **B 54**, 13009.
- Kadono R, Okajima H, Yamashita A, Ishii K, Yokoo T, Akimitsu J, Kobayashi N, Hiroi Z, Takano M and Nagamine K 1996 Phys. Rev. **B 54**, R9628.
- Katano S, Nagata T, Akimitsu J, Nishi M and Kakurai K 1999 Phys. Rev. Lett. **82**, 636.
- Kato M, Shiota K and Koike Y 1996 Physica C **258**, 284.
- Kato T, Takatsu K, Tanaka H, Shiramura W, Mori M, Nakajima K and Kakurai K 1998 J. Phys. Soc. Jpn. **67**, 752.
- Kimura T, Kuroki K and Aoki H 1996a Phys. Rev. **B 54** R9608.
- Kimura T, Kuroki K and Aoki H 1996b cond-mat/9610200.
- Kishine J and Yonemitsu K 1998 cond-mat/9802185.
- Kivelson SA, Rokhsar DS and Sethna JP 1987 Phys. Rev. **B 35**, 8865, and references therein.
- Kojima K, Keren A, Luke GM, Nachumi B, Wu WD, Uemura YJ, Azuma M and Takano M 1995 Phys. Rev. Lett. **74**, 2812.
- Konik R, Lesage F, Ludwig AWW and Saleur H 1998 cond-mat/9806334.
- Kumagai K, Tsuji S, Kato M and Koike Y 1997 Phys. Rev. Lett. **78**, 1992.
- Kurniawan B, Tanaka H, Takatsu K, Shiramura W, Fukuda T, Nojiri H and Motokawa M 1999 Phys. Rev. Lett. **82**, 1281.
- Kuroki H and Aoki H 1994 Phys. Rev. Lett. **72** 2947.
- Laukamp M, Martins GB, Gazza C, Malvezzi A, Dagotto E, Hansen P, Lopez A and Riera J 1998 Phys. Rev. **B 57**, 10755.
- Lemmens P, Fischer M, Els G, Güntherodt G, Mishchenko AS, Weiden M, Hauptmann R, Geibel C and Steglich F 1998 cond-mat/9810062.
- Levy B 1996 Physics Today (October) page 17.
- Lin HH, Balents L and Fisher MPA 1997 Phys. Rev. **B 56** 6569.
- Lin HH, Balents L and Fisher MPA 1998 cond-mat/9804221.
- Mc Carron EM, Subramanian MA, Calabrese JC and Harlow RL 1988 Mater. Res. Bull. **23**, 1355.
- Magishi K, Matsumoto S, Kitaoka Y, Ishida K, Asayama K, Uehara M, Nagata T and Akimitsu J 1998 Phys. Rev. **B 57**, 11533.
- Martin-Delgado MA, Shankar R and Sierra G 1996 Phys. Rev. Lett. **77** 3443.
- Martins G, Dagotto E and Riera J 1996 Phys. Rev. **B 54**, 16032.
- Martins G, Laukamp M, Riera J and Dagotto E 1997 Phys. Rev. Lett. **78** , 3563.
- Martins G, Gazza C and Dagotto E 1999 Phys. Rev. **B 59**, 13596.
- Matsuda M, Katsumata K, Eisaki H, Motoyama N, Uchida S, Shapiro SM and Shirane G 1996 Phys. Rev. **B 54**, 12199.
- Matsuda M, Katsumata K, Osafune T, Motoyama N, Eisaki H, Uchida S, Yokoo T, Shapiro SM, Shirane G and Zarestky JL 1997 cond-mat/9709203, preprint.
- Matsuda M, Yoshihama T, Kakurai K and Shirane G 1998 cond-mat/9808083.
- Matsuda M, Katsumata K, Eccleston R, Brehmer S and Mikeska H.-J. 1999 preprint.

- Matsumoto S, Kitaoka Y, Ishida K, Asayama K, Hiroi Z, Kobayashi N and Takano M 1996 Phys. Rev. **B 53**, 11942.
- Mayaffre H, Auban-Senzier P, Nardone M, Jérôme D, Poilblanc D, Bourbonnais C, Ammerahl U, Dhahlenne G and Revcolevschi A 1998 Science **279**, 345.
- Millet P, Satto C, Bonvoisin J, Normand B, Penc K, Albrecht M and Mila F 1998 Phys. Rev. **B 57**, 5005.
- Mito T, Magishi K, Matsumoto S, Zheng G, Kitaoka Y, Asayama K, Motoyama N, Eisaki H and Uchida S 1998 preprint, to appear in Physica B, proceedings of the SCES98 conference, Paris.
- Miyahara S, Troyer M, Johnston DC and Ueda K 1998 cond-mat/9807127
- Miyazaki T, Troyer M, Ogata M, Ueda K and Yoshioka D 1997 J. Phys. Soc. Jpn. **66**, 2580.
- Mizokawa T, Ootomo K, Konishi T, Fujimori A, Hiroi Z, Kobayashi N and Takano M 1997 Phys. Rev. **B 55**, R13373.
- Mizokawa T, Okazaki K, Fujimori A, Osafune T, Motoyama N, Eisaki H and Uchida S 1998 preprint.
- Mizuno Y, Tohyama T and Maekawa S 1997 J. Phys. Soc. Jpn. **66**, 937; 1997 Physica C **282-287**, 991.
- Moshchalkov V, Trappeniers L and Vanacken J 1998 submitted to Europhys. Letters.
- Motome Y, Katoh N, Furukawa N and Imada M 1996 J. Phys. Soc. Jpn. **65**, 1949.
- Motoyama N, Eisaki H and Uchida S 1996 Phys. Rev. Lett. **76** 3212.
- Motoyama N, Osafune T, Kakeshita T, Eisaki H and Uchida S 1997 Phys. Rev. **B 55** R3386-R3389.
- Nagaosa N, Furusaki A, Sigrist M and Fukuyama H 1996 J. Phys. Soc. Jpn. **65**, 3724.
- Nagata T, Uehara M, Goto J, Komiya N, Akimitsu J, Motoyama N, Eisaki H, Uchida S, Takahashi H, Nakanishi T and Mori N 1997 Physica C **282-287**, 153.
- Nagata T, Uehara M, Goto J, Akimitsu J, Motoyama N, Eisaki H, Uchida S, Takahashi H, Nakanishi T and Mori N 1998a Phys. Rev. Lett. **81** 1090-1093.
- Nagata T, Fujino H, Akimitsu J, Nishi M, Kakurai K, Katano S, Hiroi M, Sera M and Kobayashi N 1998b preprint.
- Nagata T, Fujino H, Ohishi K, Akimitsu J, Katano S, Nishi M and Kakurai K 1999 preprint.
- Nakamura T and Okamoto K 1998 Phys. Rev. **B 58**, 2411.
- Nazarenko A, Moreo A, Riera J and Dagotto E 1996 Phys. Rev. **B 54** R768.
- Nersesyan AA and Tselik AM 1997 Phys. Rev. Lett. **78** 3939.
- Ng TK 1996 Phys. Rev. **B 54**, 11921.
- Noack RM, White SR and Scalapino DJ 1994 Phys. Rev. Lett. **73**, 882.
- Normand B and Rice TM 1996 Phys. Rev. **B 54**, 7180.
- Normand B, Penc K, Albrecht M and Mila F 1997 Phys. Rev. **B 56**, R5736.
- Normand B and Rice TM 1997 Phys. Rev. **B 56**, 8760.
- Normand B, Agterberg DF and Rice TM 1998 cond-mat/9812211, preprint.
- Ohsugi S, Tokunaga Y, Ishida K, Kitaoka Y, Azuma M, Fujishiro Y and Takano M 1998 preprint, to appear in Phys. Rev. B.
- Ohsugi S, Magishi K, Matsumoto S, Kitaoka Y, Nagata T and Akimitsu J 1999 Phys. Rev. Lett. **82**, 4715.
- Ohta T, Onoda M, Izumi F, Isobe M, Takayama-Muromachi E and Hewat AW 1997 J. Phys. Soc. Jpn. **66**, 3107.
- Orignac E and Giamarchi T 1998 Phys. Rev. **B 57** 5812.
- Osafune T, Motoyama N, Eisaki H and Uchida S 1997 Phys. Rev. Lett. **78**, 1980.
- Osafune T, Motoyama N, Eisaki H, Uchida S and Tajima S 1999 Phys. Rev. Lett. **82**, 1313.
- Owens FJ, Iqbal Z and Kirven D 1996 preprint.
- Park Y, Liang S and Lee TK 1998 cond-mat/9811280.
- Piekarewicz J and Shepard JR 1997 Phys. Rev. **B 56**, 5366.
- Poilblanc D, Tsunetsugu H and Rice TM 1994 Phys. Rev. **B 50**, 6511.
- Regnault LP, Boucher JP, Moudden H, Lorenzo JE, Hiess A, Ammerahl U, Dhahlenne G and Revcolevschi A 1998 cond-mat/9809009, preprint.
- Rice TM, Gopalan S and Sigrist M 1993 Europhys. Lett. **23**, 445.
- Riera J and Dagotto E 1993 Phys. Rev. **B 47** 15346.
- Riera J 1994 Phys. Rev. **B 49** 3629.
- Riera J, Poilblanc D and Dagotto E 1999 Eur. Phys. J. **B 7**, 53.
- Rojo A 1996 Phys. Rev. **B 53** 9172.
- Ruzicka B, Degiorgi L, Ammerahl U, Dhahlenne G and Revcolevschi A 1998 Eur. Phys. J. **B6** 301.
- Sandvik AW, Dagotto E and Scalapino DJ 1997 Phys. Rev. **B 56**, 11701.
- Sato T, Yokoya T, Takahashi T, Uehara M, Nagata T, Goto J and Akimitsu J 1997 preprint, to be published in J. Phys. Chem. Solids.
- Schmeltzer D and Bishop AR 1998 Phys. Rev. **B 57** 5419.
- Schulz H 1996 Phys. Rev. **B 53** R2959.
- Shiramura W, Takatsu K, Tanaka H, Kamishima K, Takahashi M, Mitamura H and Goto T 1997 J. Phys. Soc. Jpn. **66**, 1900.
- Sigrist T, Schneemeyer LF, Sunshine SA, Waszczak JV and Roth RS 1988 Mater. Res. Bull. **23**, 1429.
- Sierra G, Martin-Delgado MA, Dukelsky J, White SR and Scalapino DJ 1998 Phys. Rev. **B 57** 11666.
- Sigrist M, Rice TM and Zhang FC 1994 Phys. Rev. **B 49**, 12058.
- Smolinski H, Gros C, Weber W, Peuchert U, Roth G, Weiden M and Geibel C 1998 Phys. Rev. Lett. **80**, 5164.
- Syljuasen OF, Chakravarty S and Greven M 1997 Phys. Rev. Lett. **78** 4115.
- Takahashi T, Yokoya T, Ashihara A, Akaki O, Fujisawa H, Chainani A, Uehara M, Nagata T, Akimitsu J and Tsunetsugu H 1997 Phys. Rev. **B 56**, 7870.

Takatsu K, Shiramura W and Tanaka H 1997 J. Phys. Soc. Jpn. **66**, 1611.  
Takenaka K, Mizuhashi K, Takagi H and Uchida S 1994 Phys. Rev. **B 50**, 6534.  
Takigawa M, Motoyama N, Eisaki H and Uchida S 1998 Phys. Rev. **B 57**, 1124.  
Tanaka H, Takatsu K, Shiramura W and Ono T 1996 J. of Phys. Soc. Jpn. **65**, 1945.  
Thurber K, Imai T, Saitoh T, Azuma M, Takano M and Chou F C 1999 cond-mat/9906141, preprint.  
Troyer M, Tsunetsugu H and Würtz D 1994 Phys. Rev. **B 50**, 13515.  
Troyer M, Tsunetsugu H and Rice TM 1996 Phys. Rev. **B 53**, 251.  
Troyer M, Zhitomirsky M and Ueda K 1997 Phys. Rev. **B 55**, R6117.  
Tsuiji S, Kumagai K, Kato M and Koike Y 1996 J. Phys. Soc. Jpn. **65**, 3474.  
Tsunetsugu H, Troyer M and Rice TM 1994 Phys. Rev. **B 49**, 16078.  
Tsunetsugu H, Troyer M and Rice TM 1995 Phys. Rev. **B 51**, 16456.  
Uchida S, Ido T, Takagi H, Arima T, Tokura Y and Tajima S 1991 Phys. Rev. **B 43**, 7942.  
Uehara M, Nagata T, Akimitsu J, Takahashi H, Mori N and Kinoshita K 1996 J. Phys. Soc. Jpn. **65**, 2764.  
Weihong Z, Singh RRR and Oitmaa J 1997 Phys. Rev. **B 55**, 8052.  
White SR, Noack RM and Scalapino DJ 1994 Phys. Rev. Lett. **73**, 886.  
Yamaji K and Shimoi Y 1994 Physica C **222** 349.  
Zhai Z, Patanjali P, Hakim N, Sokoloff J, Sridhar S, Ammerahl U, Vietkine A and Revcolevschi A 1999 cond-mat/9903198, preprint.

This figure "fig1.gif" is available in "gif" format from:

<http://arxiv.org/ps/cond-mat/9908250v1>

This figure "fig2.gif" is available in "gif" format from:

<http://arxiv.org/ps/cond-mat/9908250v1>



This figure "fig3.gif" is available in "gif" format from:

<http://arxiv.org/ps/cond-mat/9908250v1>

This figure "fig4.gif" is available in "gif" format from:

<http://arxiv.org/ps/cond-mat/9908250v1>

This figure "fig5.gif" is available in "gif" format from:

<http://arxiv.org/ps/cond-mat/9908250v1>

This figure "fig6.gif" is available in "gif" format from:

<http://arxiv.org/ps/cond-mat/9908250v1>

This figure "fig7.gif" is available in "gif" format from:

<http://arxiv.org/ps/cond-mat/9908250v1>

This figure "fig8.gif" is available in "gif" format from:

<http://arxiv.org/ps/cond-mat/9908250v1>

This figure "fig9.gif" is available in "gif" format from:

<http://arxiv.org/ps/cond-mat/9908250v1>

This figure "fig10.gif" is available in "gif" format from:

<http://arxiv.org/ps/cond-mat/9908250v1>



This figure "fig11.gif" is available in "gif" format from:

<http://arxiv.org/ps/cond-mat/9908250v1>

This figure "fig12.gif" is available in "gif" format from:

<http://arxiv.org/ps/cond-mat/9908250v1>

This figure "fig13.gif" is available in "gif" format from:

<http://arxiv.org/ps/cond-mat/9908250v1>

This figure "fig14.gif" is available in "gif" format from:

<http://arxiv.org/ps/cond-mat/9908250v1>

This figure "fig15.gif" is available in "gif" format from:

<http://arxiv.org/ps/cond-mat/9908250v1>

This figure "fig16.gif" is available in "gif" format from:

<http://arxiv.org/ps/cond-mat/9908250v1>

This figure "fig17.gif" is available in "gif" format from:

<http://arxiv.org/ps/cond-mat/9908250v1>

This figure "fig18.gif" is available in "gif" format from:

<http://arxiv.org/ps/cond-mat/9908250v1>



This figure "fig19.gif" is available in "gif" format from:

<http://arxiv.org/ps/cond-mat/9908250v1>

This figure "fig20.gif" is available in "gif" format from:

<http://arxiv.org/ps/cond-mat/9908250v1>

This figure "fig21.gif" is available in "gif" format from:

<http://arxiv.org/ps/cond-mat/9908250v1>

This figure "fig22.gif" is available in "gif" format from:

<http://arxiv.org/ps/cond-mat/9908250v1>

This figure "fig23.gif" is available in "gif" format from:

<http://arxiv.org/ps/cond-mat/9908250v1>

This figure "fig24.gif" is available in "gif" format from:

<http://arxiv.org/ps/cond-mat/9908250v1>

This figure "fig25.gif" is available in "gif" format from:

<http://arxiv.org/ps/cond-mat/9908250v1>

This figure "fig26.gif" is available in "gif" format from:

<http://arxiv.org/ps/cond-mat/9908250v1>



This figure "fig27.gif" is available in "gif" format from:

<http://arxiv.org/ps/cond-mat/9908250v1>

This figure "fig28.gif" is available in "gif" format from:

<http://arxiv.org/ps/cond-mat/9908250v1>

This figure "fig29.gif" is available in "gif" format from:

<http://arxiv.org/ps/cond-mat/9908250v1>

This figure "fig30.gif" is available in "gif" format from:

<http://arxiv.org/ps/cond-mat/9908250v1>

This figure "fig31.gif" is available in "gif" format from:

<http://arxiv.org/ps/cond-mat/9908250v1>

This figure "fig32.gif" is available in "gif" format from:

<http://arxiv.org/ps/cond-mat/9908250v1>

This figure "fig33.gif" is available in "gif" format from:

<http://arxiv.org/ps/cond-mat/9908250v1>

This figure "fig34.gif" is available in "gif" format from:

<http://arxiv.org/ps/cond-mat/9908250v1>



This figure "fig35.gif" is available in "gif" format from:

<http://arxiv.org/ps/cond-mat/9908250v1>

This figure "fig36.gif" is available in "gif" format from:

<http://arxiv.org/ps/cond-mat/9908250v1>

This figure "fig37.gif" is available in "gif" format from:

<http://arxiv.org/ps/cond-mat/9908250v1>

This figure "fig38.gif" is available in "gif" format from:

<http://arxiv.org/ps/cond-mat/9908250v1>

This figure "fig39.gif" is available in "gif" format from:

<http://arxiv.org/ps/cond-mat/9908250v1>

This figure "fig40.gif" is available in "gif" format from:

<http://arxiv.org/ps/cond-mat/9908250v1>

This figure "fig41.gif" is available in "gif" format from:

<http://arxiv.org/ps/cond-mat/9908250v1>